ERDC TR-19-16

US Army Corps
of Engineers®
Engineer Research and
Development Center

ERDC
ENGINEER RESEARCH & DEVELOPMENT CENTER

Monitoring Completed Navigation Projects (MCNP) Program
Navigation Systems (NavSys) Research Program

Feasibility of Discontinuous Quoin Blocks for USACE Miter Gates

Brian A. Eick, Matthew D. Smith, and Travis B. Fillmore

July 2019

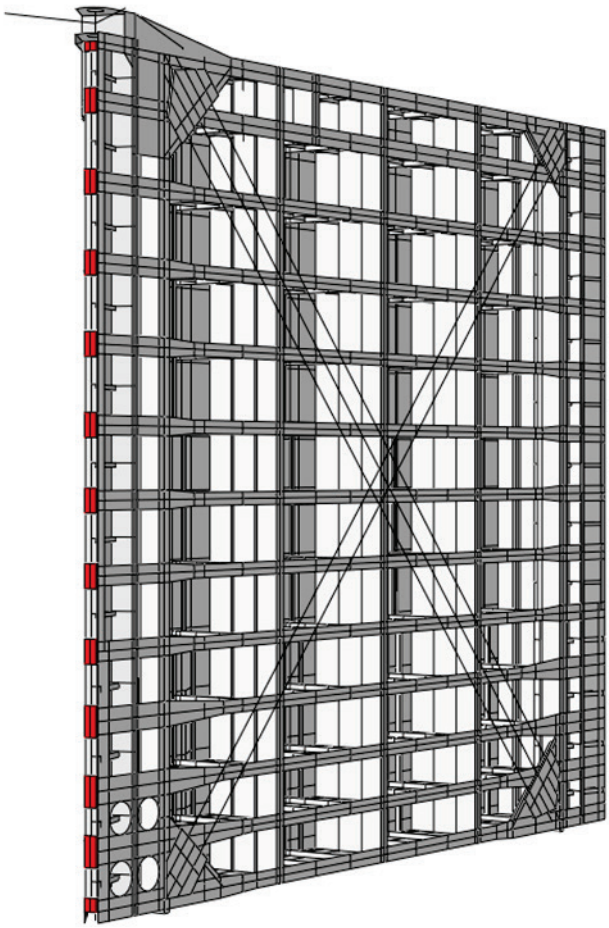

Engineer Research and
Development Center

The U.S. Army Engineer Research and Development Center (ERDC) solves the nation's toughest engineering and environmental challenges. ERDC develops innovative solutions in civil and military engineering, geospatial sciences, water resources, and environmental sciences for the Army, the Department of Defense, civilian agencies, and our nation's public good. Find out more at www.erdc.usace.army.mil.

To search for other technical reports published by ERDC, visit the ERDC online library at http://acwc.sdp.sirsi.net/client/default.

Monitoring Completed Navigation Projects
(MCNP) Program
Navigation Systems (NavSys) Research Program

ERDC TR-19-16
July 2019

Feasibility of Discontinuous Quoin Blocks for USACE Miter Gates

Brian A. Eick

U.S. Army Engineer Research and Development Center
Construction Engineering Research Laboratory
2902 Newmark Drive
Champaign, IL 61822

Matthew D. Smith and Travis B. Fillmore

U.S. Army Engineer Research and Development Center
Coastal and Hydraulics Laboratory
3909 Halls Ferry Road
Vicksburg, MS 39180-6199

Final report

Prepared for Headquarters, U.S. Army Corps of Engineers
Washington, DC 20314-1000

Under Work Unit 055F4K; “Innovative Structural Health Monitoring Technologies”

Abstract

Navigation lock chambers have gates that act both as damming surfaces for water and as doorways for vessels to enter and exit. Miter gates are by far the most common type of lock gate in the U.S. Army Corps of Engineers inventory. Horizontally framed miter gates are designed to bear continuously against the lock chamber wall along the height of the gate in the region known as the quoin. To aid continuous contact along the quoin, contact blocks are installed. Currently, each contact block is effectively one continuous piece of steel, making installation difficult and requiring the entire piece to be replaced even if only part is damaged. To address these shortcomings, this study investigated using discontinuous multiple quoin blocks instead, particularly as a retrofit option. Numerical models demonstrated the new design's stress range to be within appropriate limits, making discontinuous quoin blocks a feasible design. Supplementary results indicated issues with current placement of quoin block splices, suggesting that contact block splices should not be made in line with the centerline of girder webs as is common practice.

Contents

Figures and Tables

Figures

Tables

Preface

This study was conducted for Headquarters, U.S. Army Corps of Engineers (HQUSACE) under the Monitoring Completed Navigation Projects (MCNP) Program, and the Navigation Systems (NavSys) Research Program, Work Unit 055F4K, "Innovative Structural Health Monitoring (SHM) Technologies," administered by the USACE Engineer Research and Development Center (ERDC), Coastal and Hydraulics Laboratory (CHL). At the time this study was conducted, Mr. Jeffrey A. McKee was Chief, HQUSACE Navigation Branch, and USACE Navigation Business Line Manager. Mr. W. Jeff Lillycrop, HZT, CHL, was the Technical Director for Civil Works, and Navigation Research, Development, and Technology Transfer portfolio. Dr. Lyndell Z. Hales was the CHL MCNP Program Manager, and Mr. Charles E. Wiggins was the CHL NavSys Program Manager. Mr. Matthew D. Smith, CHL, was the ERDC SHM Lead. At the time of publication of this report, the Deputy Director of CHL was Mr. Jeffrey R. Eckstein, and the Director of CHL was Dr. Ty V. Wamsley.

The work was performed by the Materials and Structures Branch, Installations Division, ERDC Construction Engineering Research Laboratory (CERL). At the time of publication of this report, Ms. Vicki Vanblaricum was Chief, Materials and Structures Branch; Mr. Donald K. Hicks was Chief, Installations Division; and Mr. Kurt J. Kinnevan, CZT, CERL, was the Technical Director for Infrastructure for Combat Operations. The Deputy Director of CERL was Dr. Kirankumar V. Topudurti, and the Director of CERL was Dr. Lance D. Hansen.

COL Ivan P. Beckman was Commander of ERDC, and the Director of ERDC was Dr. David W. Pittman.

1 Introduction

1.1 Background

The U.S. Army Corps of Engineers (USACE) operates and maintains 239 lock chambers at 193 lock sites (USACE 2016a). Each lock chamber utilizes a lock gate to control water flow. Greater than 90% of lock gates are miter lock gates, making them the most common gate type found at USACE lock and dam sites (USACE 2014b). While there are many components of miter gates, this study focuses on the region of the gate known as the quoin, which is intended to facilitate the transfer of hydrostatic load through bearing pressure against the concrete lock wall. Specifically, this study focuses on the contact blocks that are installed in the quoin region on the miter gate. For horizontal miter gates designed and operated by USACE, these contact blocks are intended to be one continuous piece of steel spanning the entire height of the quoin region of the gate. The size and rigidity of a typical continuous contact block utilized at USACE miter gates make installation and adjustment of the contact block difficult, expensive, and potentially dangerous. Moreover, repair of continuous contact blocks is needlessly expensive, since the entire block must be completely replaced if even one area becomes damaged or worn. Several international organizations already operate miter gates that are designed to utilize quoin blocks that are comprised of many small pieces of steel, herein referred to as "discontinuous" quoin blocks. This study intends to investigate the use of discontinuous quoin blocks on USACE miter gates that were designed to utilize continuous quoin blocks. By investigating the feasibility of retrofitting existing miter gates with discontinuous contact blocks, the current work models an alternative that will reduce installation and maintenance costs, facilitate adjustment of the contact blocks, as well as minimize safety concerns during installation.

Further background about a lock site's general design and operation, contact block load path, issues with continuous contact quoin blocks, and a discussion of discontinuous blocks is presented in Chapter 2.

1.2 Objective

The objective of this study is to demonstrate the feasibility of utilizing discontinuous quoin blocks on miter gates. Of particular interest is the

feasibility of utilizing discontinuous quoin blocks as a retrofit option on already-constructed miter gates in the USACE inventory. Clearly, discontinuous quoin blocks are viable when the gate has been designed specifically to utilize discontinuous quoin blocks. The research presented herein investigated the feasibility of discontinuous quoin blocks on already-built gates that were originally designed specifically to utilize continuous quoin blocks.

1.3 Approach

This study used numerical finite element analysis (FEA) models to determine the magnitude of stress in relevant sections of a group of miter gates with (a) continuous and (b) discontinuous contact blocks. An extreme load scenario was applied to the miter gate models to simulate the highest loads likely to be experienced by the physical miter gate. Additionally, boundary condition degradation (damage) scenarios, in the form of gaps in the contact surface, were also simulated to facilitate investigating the damage tolerance of discontinuous quoin blocks. Ultimately, von Mises stress in the quoin region was tabulated and compared between the continuous and discontinuous quoin cases, and recommendations are made about the feasibility of discontinuous quoin blocks as a retrofit option on USACE miter gates.

2 Background of Lock Site, Miter Gate, and Discontinuous Quoin Block Operations

2.1 Lock sites

Lock sites typically consist of a dam that is constructed to maintain a navigable depth of water and a lock chamber that works like an elevator for waterway traffic. A vessel enters the lock (Figure 1(a)), the stern gate is closed, and depending on the direction of travel, the water in the lock is either raised or drained to match the water level opposite the bow gate. In Figure 1(b), the bow gate is the upstream gate, and the stern gate is downstream. Once the water levels align, the bow gate opens, and the vessel proceeds on its route, as seen in Figure 1(c).

Figure 1. Typical lockage procedure: (a) ship enters lock, (b) gate closes and chamber water level rises, and (c) ship leaves lock.

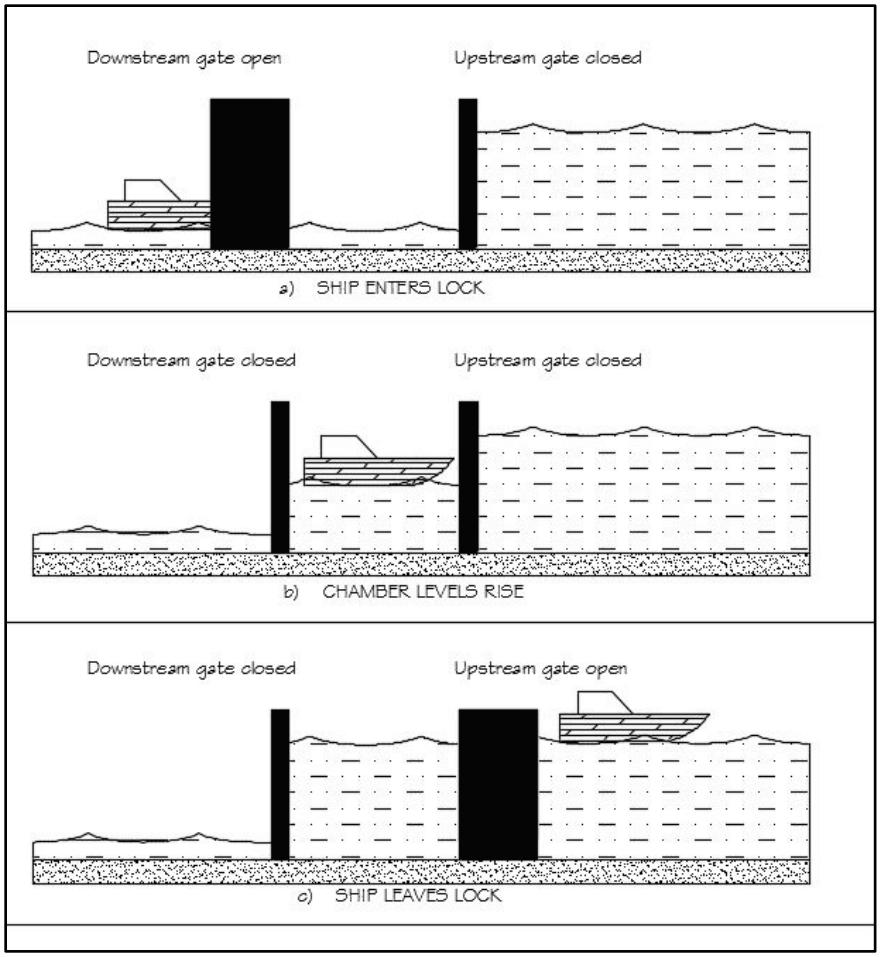

2.2 Miter gates

Characterized by their primary load-carrying members, miter gates are either vertically framed (using vertical steel girders) or horizontally framed (using horizontal steel girders). A miter gate consists of two leaves, which, when closed, are referred to as "mitered." The mitered gate primarily dams the water upstream, facilitating the lock chamber to fill or empty with water as appropriate. Figure 2 shows the typical components of a horizontally framed miter gate. The quoin is the tapered region of the gate next to the lock chamber wall and is circled in the upper diagram (plan view) in Figure 2.

Figure 2. Typical horizontally framed miter gate elevation.

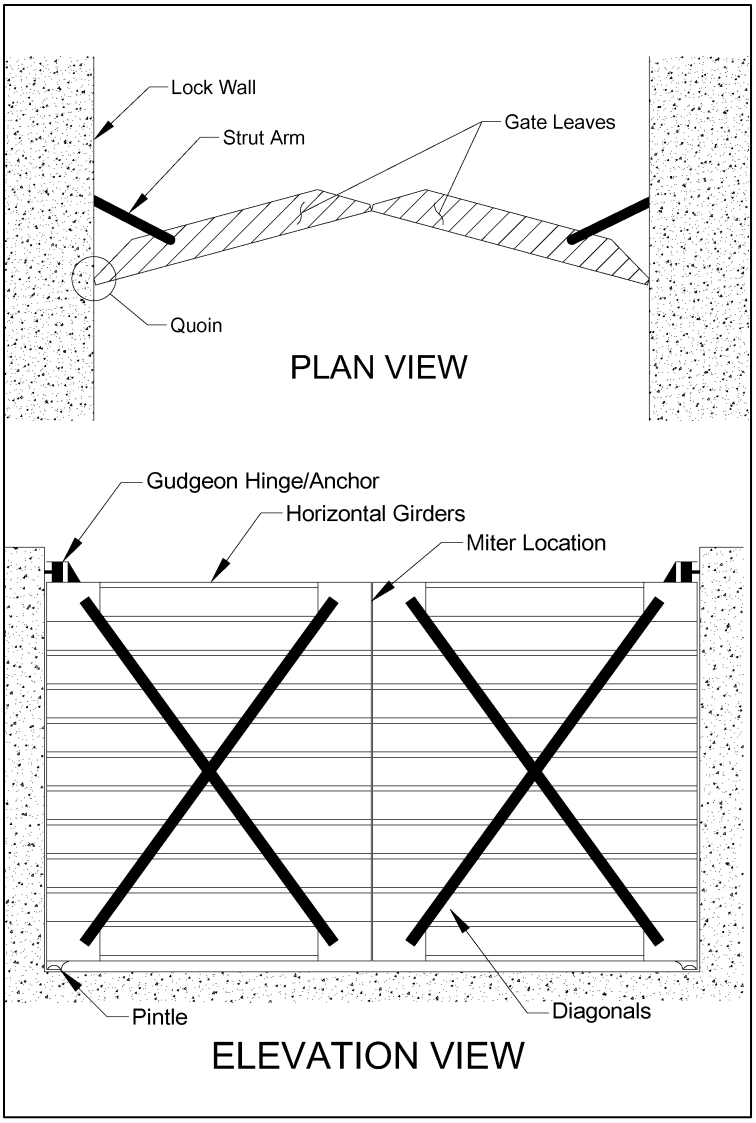

To understand the function of the contact blocks of the quoin region of miter gates, the intended load path of the gates must first be understood. The load scenario of interest for this study occurs when miter gates are subjected to a hydrostatic load. When the gate is closed and the water level differs on either side of the gate, a pressure is applied to the gate, as seen in Figure 3. Under normal operating conditions, each leaf of the gate is designed to bear continuously against a steel member embedded in the lock wall. Additionally, the gate leaves are designed to bear against each other. These boundary conditions are intended to facilitate a three-hinged arch-like behavior, with the water pressure on the gate being transferred into the lock chamber wall through axial compression of the horizontal girders. Figure 4 provides a diagram highlighting the intended load path for one leaf of a miter gate. For the intended arch-like behavior to be realized at every girder, each girder needs to be in contact with the wall when the gate is under load. To facilitate the establishment of contact at each girder, the contact block on the gate is adjustable during installation.

Figure 3. Typical loading scenario for a miter gate.

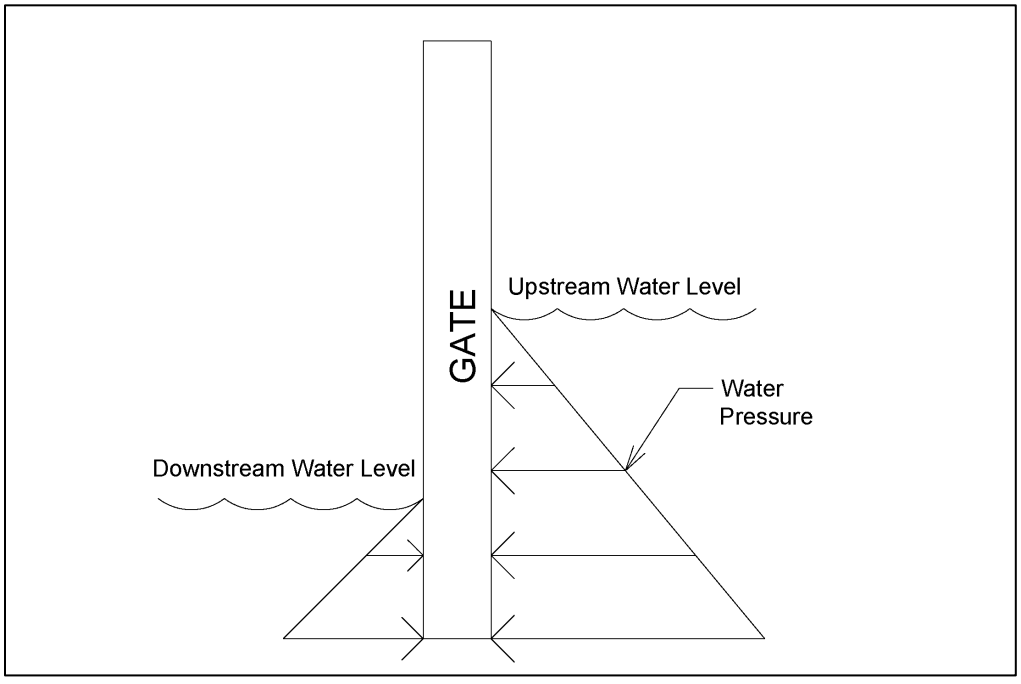

Figure 4. Intended load path for miter gates.

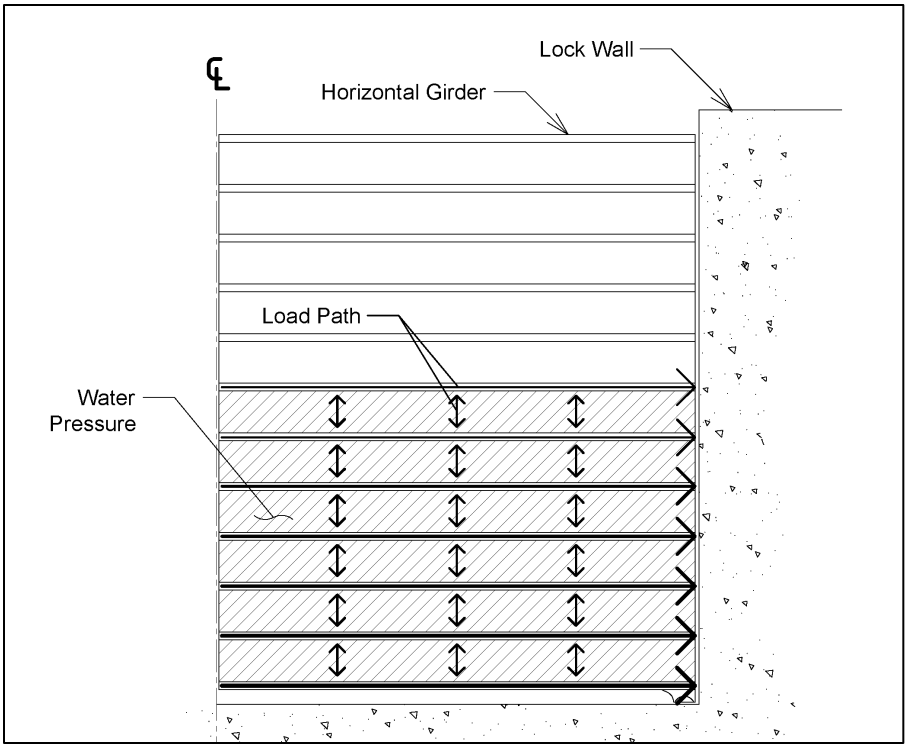

2.2.1 Contact blocks

Typical miter gate construction involves the fabrication and installation of contact blocks that are effectively a buffer between the concrete chamber wall and the gate itself. Design of contact blocks in the USACE inventory is governed by the USACE Engineering Technical Letter 1110-2-584 (USACE 2014a), which is similar to the previous governing design document USACE Engineering Manual (EM) 1110-2-2703 (USACE 1994), herein referred to as simply "the EM." An overview of international opinion on contact block design can be found in the more recent PIANC report on miter gate design (PIANC 2017). Both documents give general recommendations on block shapes and installation procedures, an overview of which will be presented here.

The EM (USACE 1994) notes that the contact blocks serve two functions. First, contact blocks facilitate an even distribution of the intended thrusting load from the gate into the lock chamber wall. Second, they act as a seal between the gate and the wall. Generally, contact blocks are solid steel elements with typical dimensions on the order of 3–4 inches (in.) thick and 8–10 in. wide. Contact blocks are intended to span the entire height of the gate (typically 600–800 in.), but for constructability

purposes, they are typically allowed to be fabricated in large, individual pieces that are then spliced together. For example, the structural drawings for the Mississippi River Lock 27 miter gate call for three separate contact block pieces, each approximately 24 feet (ft) long, to be spliced together in the field. Note that the EM (USACE 1994) calls for these splices to occur at the centerline of horizontal girders. This suggestion was applied to the Lock 27 design and is duly noted on the structural drawing. The appropriateness of the suggested location of this splice is investigated in Chapter 6.

Contact blocks in the United States are typically flat on the back side to facilitate load transfer to the gate, and they are convex on the side that will contact the wall. Along the wall, a concave steel member is embedded, against which the gate's contact block bears. This configuration allows for contact at a very small point and facilitates the gate's swing action. This typical geometry is seen in the cross-sectional plan view of a contact block in Figure 5. It has been noted in the PIANC report, however, that international opinion on the preferred geometry of contact blocks varies greatly (PIANC 2017).

Figure 5. Typical contact block cross-section detail.

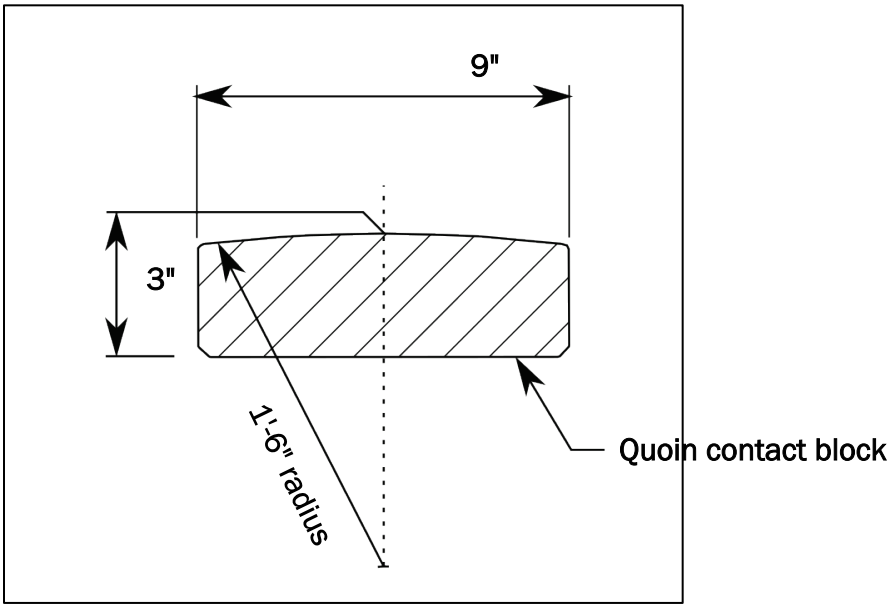

Because of fabrication irregularities and potential warping of the large contact blocks, a procedure is generally followed to allow adjustment of the contact blocks and ensure continuous contact along the height of the quoin. A typical adjustment strategy is to apply a pair of push and pull

screws along the height of the block, as noted in the EM (USACE 1994). Figure 6 shows a plan view of the quoin-block end of a girder, highlighting the typical bolt arrangement for the quoin block. As seen, there is generally one bolt threaded into the contact block that is used to pull the block towards the gate. Opposite the threaded bolt, there is typically a cap screw that is used to push the block toward the lock chamber wall. A typical layout for these push-pull screws is to apply them every 2 ft along the height of the quoin, as shown in the turned elevation view in Figure 6 (bottom left).

Figure 6. Plan view showing cap screw, attachment bolt, and epoxy filler (bottom right); bottom left: elevation view showing zig-zag pattern of bolts on quoin block.

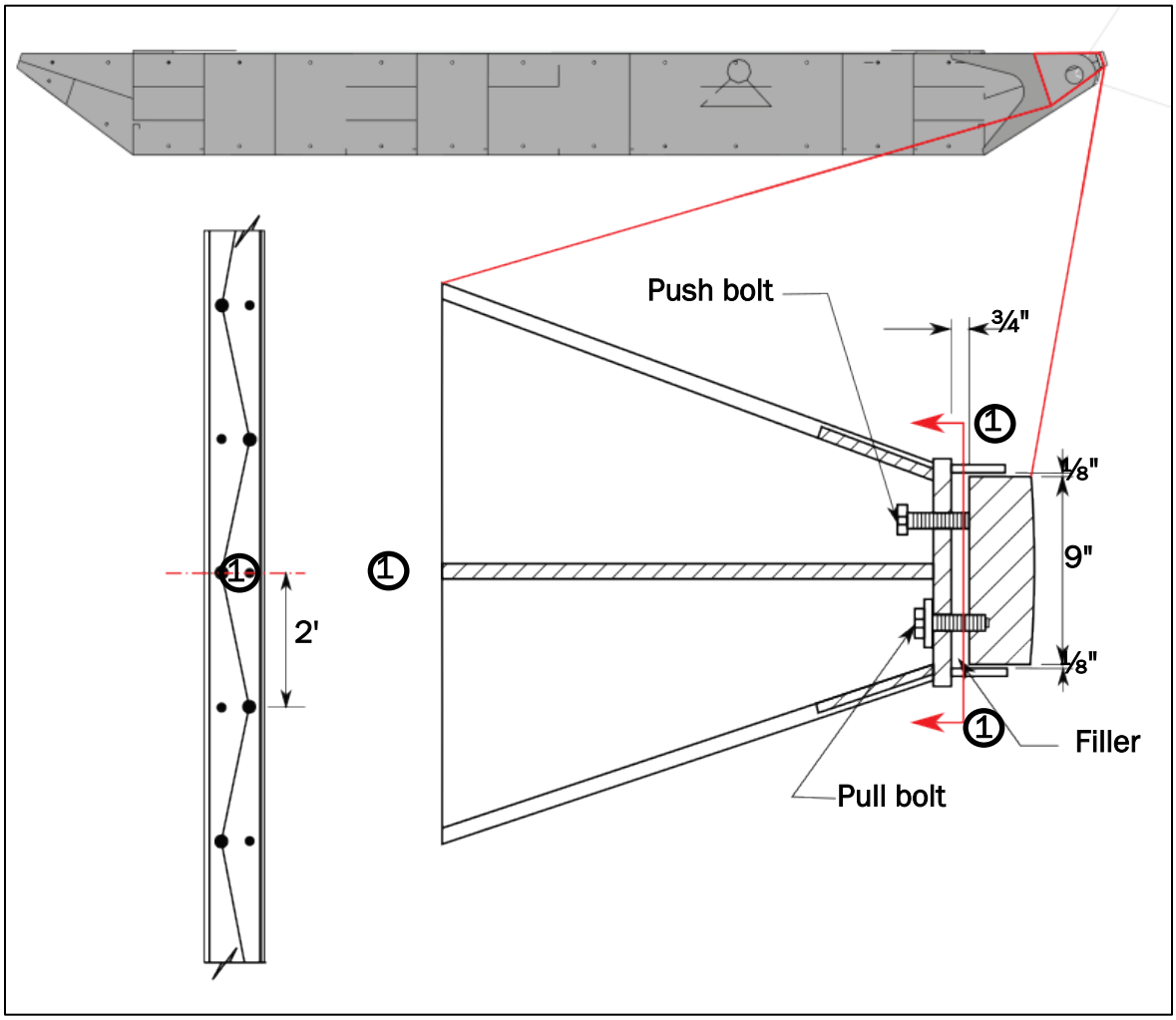

The threaded pull bolts serve the additional function of physically attaching the block to the gate; however, the need for adjustability dictates the requirement of a gap between the contact block and the gate. To further ensure the even distribution of contact pressure from the contact

block into the end plate of the gate, an epoxy or molten zinc is added in this small gap to prevent all the load transfer through the sparse array of bolts. The small gap and epoxy filler location are shown in Figure 6. Typically, the quoin block is fully adjusted by using the push-pull screws so that contact is present to within the desired tolerances; then the backing material is added. The PIANC report (2017) notes that there are several other options for contact block adjustability, such as the use of steel shims instead of push-pull bolts.

2.2.2 Stress distribution in contact blocks

One of the primary motivations for the installation of continuous quoin blocks is the notion that a continuous quoin block facilitates an even distribution of stress throughout the quoin region. However, previous modeling efforts (Eick et al. 2018) have highlighted that the quoin block does not provide an even stress distribution. Figure 7(a) provides an elevation view of the gate that was modeled using the commercial software Abaqu. The gate model was subjected to a hydrostatic load that would be typical for the location, and the stress was extracted for the location of the quoin immediately next to the gate-to-wall contact surface; Figure 7(b) shows the von Mises stress distributions along the height of the quoin. The y-axis corresponds to the height along the quoin from the bottom girder, while the x-axis corresponds to the magnitude of the von Mises stress. The horizontal dotted lines are added to the plot to illuminate the locations along the height of the quoin that align with the centerline of the horizontal girders on the gate.

In Figure 7(b), it is seen that the highest concentrations of stress in the quoin occur at the girder center lines and diminish between girders. Figure 7 highlights that the quoin block appears to have very little function between girders; therefore, the presumed function of providing an even distribution of stress throughout the quoin region is not fully achieved.

Figure 7. (a) Elevation view of Greenup gate and (b) von Mises stress distribution along height of quoin.

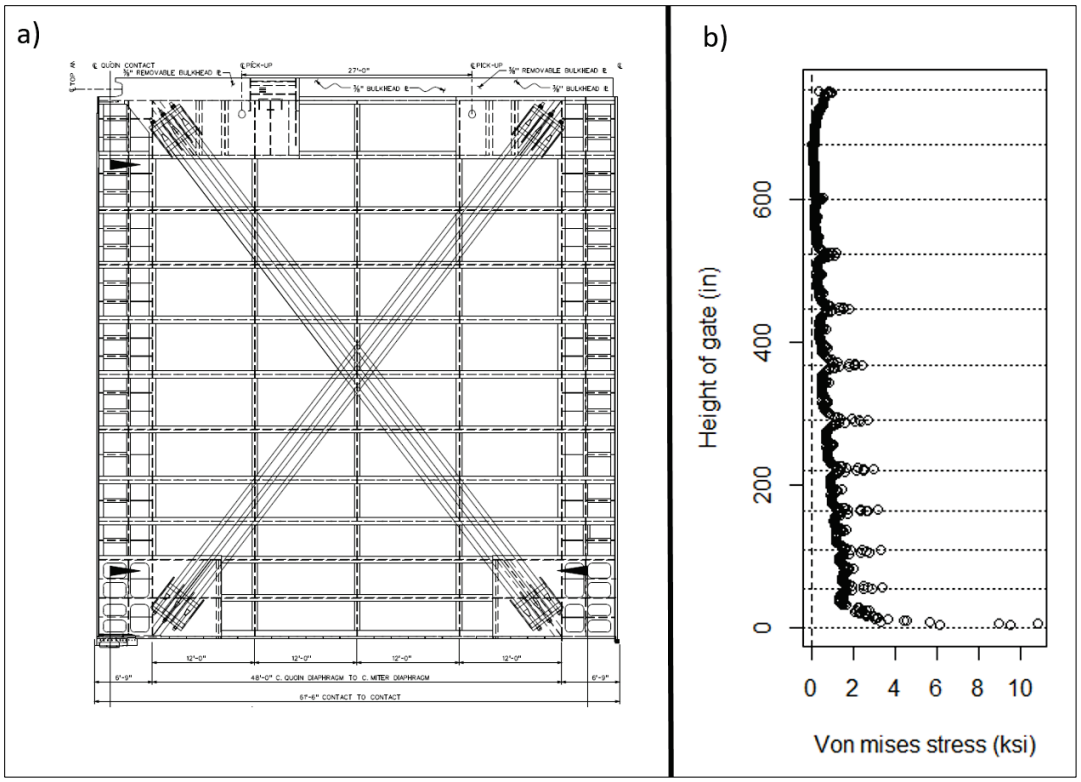

2.2.3 Issues with continuous quoin blocks

The continuous nature of typical contact blocks of miter gates causes many issues. One of the main issues is their weight. If steel has a unit weight of 490 pounds (lb) per cubic foot, then steel blocks of the dimensions given in the previous section would have a weight of between 4,000 and 9,000 lb. Even if they are cut into thirds, as allowed in the Lock 27 structural drawings, the weight of the blocks would still require the use of a crane, and installation could pose a safety risk for installers. Furthermore, when the contact block degrades and needs to be replaced, the continuous nature of the block dictates that the entire piece be replaced, even if only a small portion of that piece has been damaged.

Figure 8 shows an example of a damaged quoin block found at the Captain Anthony Meldahl Lock and Dam on the Ohio River. In this scenario, the quoin block became damaged for an unknown reason, causing the quoin block below the arrow to fall off the gate. The loss of contact between the gate and the chamber wall prevented the gate from properly developing the desired arch-like action. The resulting alternative load path caused significant cracking in the pintle region, as seen in Figure 9.

Figure 8. Quoin area of the miter gate, located at the Captain Anthony Meldahl Locks and Dam, showing the entire quoin block missing.

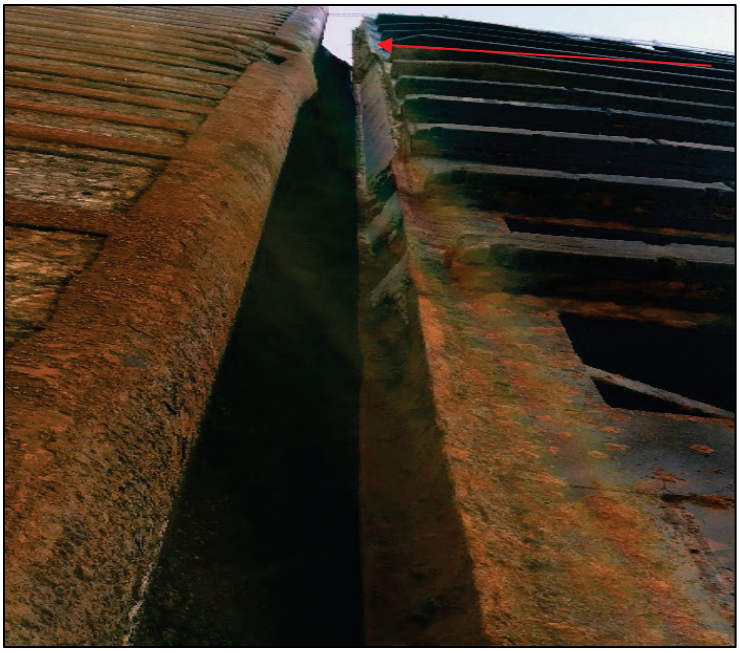

Figure 9. Cracking in the pintle area of a miter gate at the Captain Anthony Meldahl Locks and Dam.

It has been noted that continuous quoin blocks are difficult to adjust to obtain perfect contact along the height of the quoin (PIANC 2017). This difficulty is due to the typical arrangement of push-pull screws at sparse

intervals along the height of the very stiff quoin block. Obtaining uniform load distribution from the contact block to the actual gate requires a uniform and void-free placement of the epoxy filler between the contact block and the gate. Conversations with USACE design engineers[1] and a publication by the USACE lock operations community of practice (USACE 2016b) highlighted the difficulty of pouring the backing material into a very long channel and also ensuring a uniform distribution. Also, there is currently no requirement nor method for inspection of the backing material to test for voids. Similarly, if a void were found, there is no method nor requirement to address the issue. Finally, once the backing material is poured, it is difficult to further adjust the contact blocks should they initially be improperly adjusted, the blocks wear down, or some other change misaligns the blocks.

2.3 Discontinuous quoin blocks

To address the shortcomings in using continuous quoin blocks, the research presented herein investigated the use of discontinuous quoin blocks. For this study, a discontinuous quoin block is defined as a block made up of individual pieces that are placed at the ends of the lock gate girders. The lengths of the individual pieces are equal to the flange widths of the gate's girders, plus 2 in. on either side of the flange. Figure 10 depicts a single miter gate leaf, with both continuous and discontinuous quoin blocks shown in red. Figure 10(a) shows the continuous quoin block while Figure 10(b) shows the discontinuous quoin block, with pieces of quoin block only located at locations where the end of a girder meets the quoin block.

The discontinuous quoin block pieces are significantly smaller than the continuous quoin block. A typical flange width for a miter gate girder is 12 in., so with a 2 in. overhang on either side, a discontinuous quoin block piece would only be 16 in. long, in stark contrast to the 288 in. minimum allowed by the Lock 27 structural drawings. A 16 in. block piece would only weigh a little over 100 lb, making it entirely feasible to install the piece without a crane. Moreover, if a discontinuous quoin block piece fails, only a small portion of the gate will be affected, and replacement would require a less significant effort. Replacement could also be performed without the

[1] Teleconference with Andy Harkness, Fred Joers, Eric Johnson, and Paul Surace of the Inland Navigation Design Center, spring 2018.

need to dewater the entire lock chamber, providing significant cost savings.

Discontinuous quoin blocks not only make maintenance easier, they also facilitate damage detection. First, a much smaller section of the quoin block needs to be monitored. Second, the load paths are focused through each girder to the discontinuous quoin block section more than for the continuous case. Thus, strain gages in a structural health monitoring system can more easily detect change in strain, resulting from increases in stress, resulting from damage in the discontinuous quoin block sections.

Overall, a discontinuous quoin block retrofit enables engineers to more efficiently maintain the quoin block through improved damage detection, readjustment, and replacement. Further improvements to the quoin could involve the use of composite materials to mitigate fatigue and corrosion effects, and this research is part of other current efforts.

Figure 10. Continuous quoin block (a), and discontinuous quoin block (b).

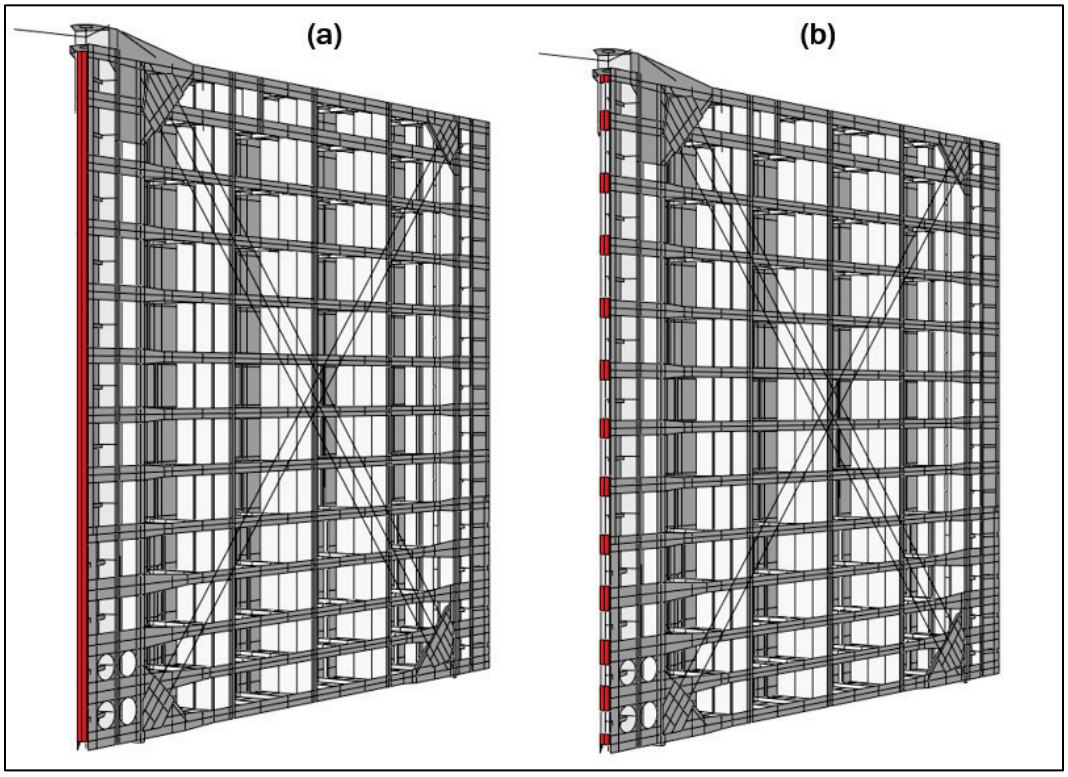

Discontinuous, or intermittent, contact blocks are not necessarily a novel idea. A PIANC report of miter gate design notes that they are a viable option for newly designed miter gates, but does not provide additional details (PIANC 2017). Similarly, discontinuous quoin blocks have also already found use in Europe, where several gates have been designed to utilize this feature, as referenced in a study by Daniel (2000). Figure 11 is an overhead view of the quoin region of the Diepenbeek locks in Belgium, showing the discontinuous contact surfaces. Figure 12 is looking downward on an angle at the quoin region of a miter gate on the Dnieper River in Ukraine, and it shows similar discontinuous contact surfaces.

Figure 11. Top view of quoin region of Diepenbeek lock, Belgium, showing discontinuous contact regions.

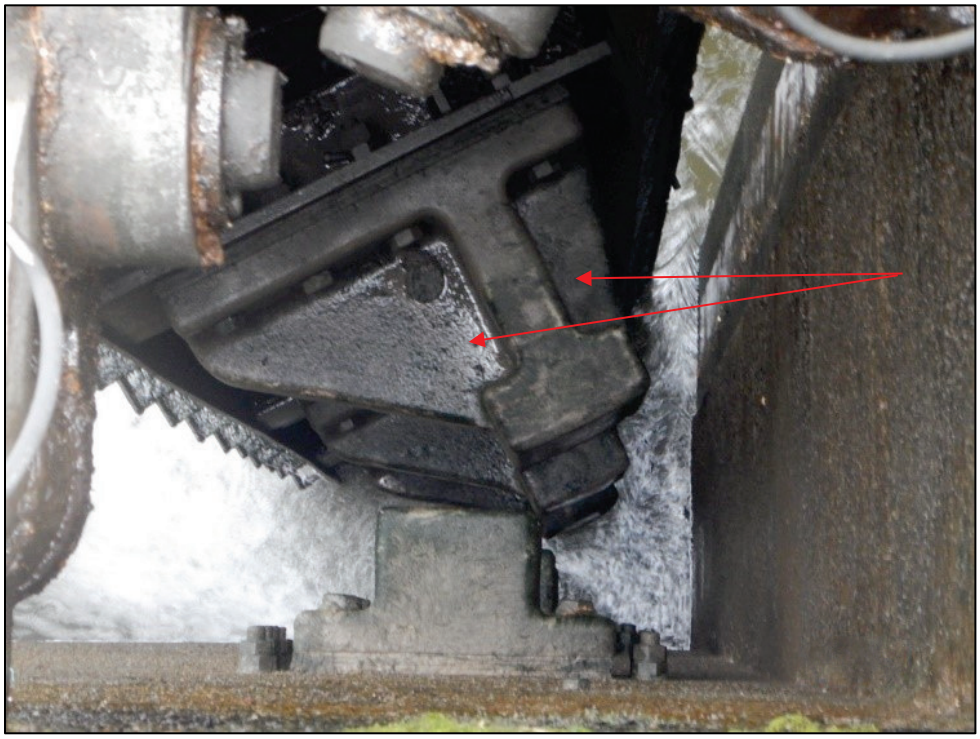

Figure 12. Locks on the Dnieper River, Ukraine, showing intermittent contact surfaces.

An issue with the use of discontinuous quoin blocks that has yet to be discussed is in regards to their secondary function—namely, sealing the upstream water from seepage. Gate examples in Figure 11 and Figure 12 show that a supplementary seal is used in place of a continuous quoin. A large rubber seal is placed on the upstream side of the quoin block. An example of this was found at the Diepenbeek Lock and is shown in Figure 13. The orange piece seen on the end of the gate is the supplementary wooden seal. This gate has been operated without issues, so the concern of sealing the quoin region of the gate will not be discussed further in this report.

Figure 13. Supplementary water seal at Diepenbeek lock.

3 Methodology

This section describes the analysis that was performed to investigate the feasibility of using discontinuous quoin blocks. The analysis was exclusively done using numerical models in the Abaqus commercial FEA software. A brief description of the FEA models utilized for this analysis is given herein.

3.1 Gate models

A selection of representative lock gates have been modeled in the Abaqus FEA software, as listed in Table 1. Miter gate design within USACE is not standardized, creating many different design-types for miter gates in the USACE inventory. Under guidance from the USACE Inland Navigation Design Center (INDC), the lock gates modeled and listed in Table 1 were selected with the intention of their being representative of a large percentage of miter gates found in the USACE inventory. Lock 27 is intended to be representative of the horizontally framed miter gates found on the Upper Mississippi River. Greenup is intended to be representative of newer lock gates designed by the USACE Huntington District and found on the Ohio River while Racine is intended to be representative of the older gates designed by Huntington. Cannelton is representative of newer gates designed by the Louisville District and also found on the Ohio. Terry is intended to represent the shorter gates with a larger aspect ratio found throughout the USACE inventory. Lockport is intended to be representative of gates found on the Illinois River. Through conversations with the INDC, the models selected are estimated to be nominally representative of some 80% of all horizontally framed miter gates found in the United States.

Table 1. Modeled lock gates.

Model	Location
Lock 27	Mississippi River
Greenup	Ohio River
Terry	Arkansas River
Cannelton	Ohio River
Racine	Ohio River
Lockport	Illinois River

The models were created in Abaqus, and the geometry was input based on as-built structural drawings obtained from USACE engineers. The model was constructed as a three-dimensional (3D) shell model, due to the shell-like nature of the gate's components, while the diagonals and anchor bars were added using beams. The quad-dominated mesh control was assigned to the entire gate, which leads to a mesh consisting primarily of S4R linear quadrilateral elements but also allows the use of S3 linear triangular elements where complicated geometry dictates their necessity. As a typical example, the Greenup model consists of 380,565 elements, of which 1,904 elements are linear line B31 elements, 20,661 are triangular S3, and the remaining 358,000 elements are quadrilateral S4R. For all models, a linear elastic material model was used to represent steel. The modulus of elasticity was set at 29,000 kips/square inch (ksi) while the Poisson ratio was set at 0.3. No other material properties were needed for this analysis.

3.2 Lock 27 loads considered

Of particular interest to this study is investigating the change in stress distribution in a lock gate between a scenario in which the gate has a continuous quoin block and a scenario in which the gate has a discontinuous quoin block. For this study, the gate models will only be subjected to hydrostatic load, as this load case is the only time the quoin blocks provide their intended function. Furthermore, an extreme hydrostatic load will be simulated to attempt to determine the worst possible effects that can be expected on a particular lock gate due to a discontinuous quoin block. Through conversations with the USACE design engineers,[1] an appropriate extreme loading scenario for a miter gate would be one in which a hydrostatic load that is equivalent to a column of water with a height of 85% of the lock gate height is applied to the upstream side, and a column of water with a height of 15% of the lock gate height is applied to the downstream side (with all heights rounded to the nearest inch). This load scenario is shown in Figure 14. Table 2 shows the numbers used to apply the hydrostatic load in Abaqus. These are provided for ease of the reader to facilitate reproduction of the work. Input of a hydrostatic load in Abaqus requires a magnitude and a height. The magnitudes in Table 2 correspond to the pressure at the bottom of the gate. The exception to this scenario is Lock 27, as explained in subsection 3.2.1.

[1] Teleconference between the authors and Andy Harkness, Fred Joers, Eric Johnson, and Paul Surace of the Inland Navigation Design Center of USACE, spring 2018.

Figure 14. Loading scenario used for all analyses.

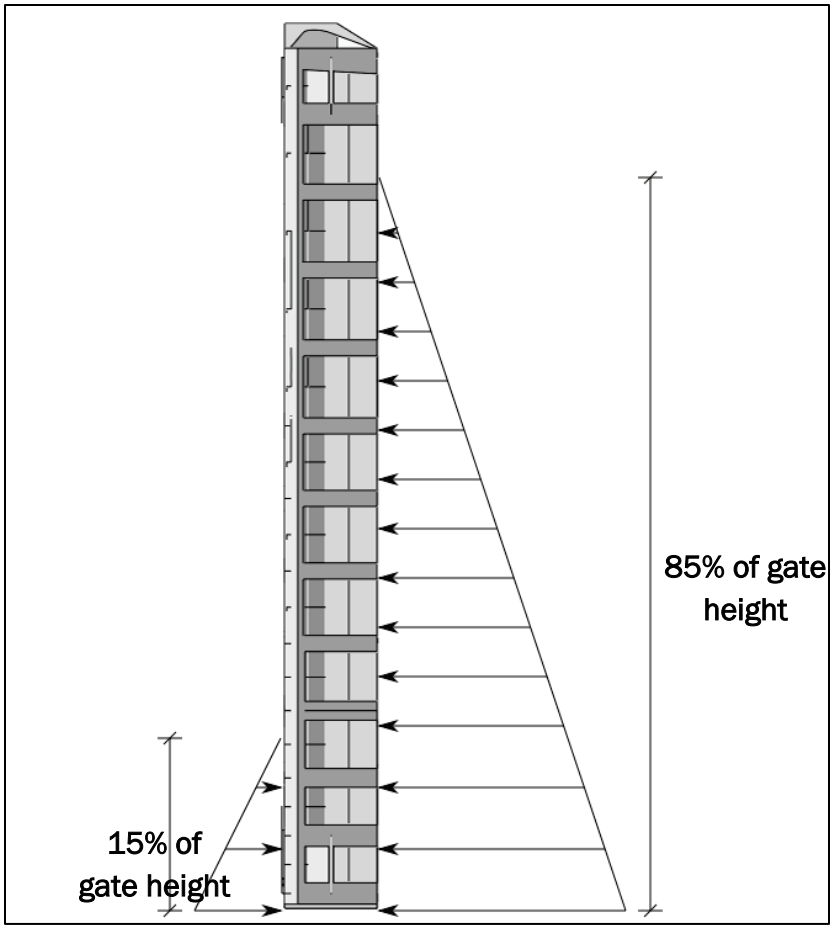

Table 2. Hydrostatic load height and magnitude.

Model	Upstream Height	Upstream Magnitude (ksi)	Downstream Height	Downstream Magnitude (ksi)
Greenup	53'-11"	0.023	9'-7"	0.0042
Cannelton	47'-1"	0.020	8'-4"	0.0036
Lock 27*	47'-0"	0.020	32'-0"	0.0139
Terry	33'-1"	0.014	6'-2"	0.0027
Racine	41'-6"	0.018	7'-9"	0.0034
Lockport	47'-3"	0.021	8'-11"	0.0038

*Lock 27 load was reduced because of modeling issues.

For Lock 27, this load scenario proved to be too extreme, and it led to significant modeling issues. For Lock 27, the historical water levels at the lock were investigated, and it was found that the lock gate is almost never subjected to a differential head load of more than 10 ft. This is seen in Figure 15, which shows a plot of the upstream and downstream water

levels seen at Lock 27 in 2014. The upstream water level is the black line while the downstream water level is the blue line. The change in water level in the lock chamber, and thus the load placed on the gate, is exactly equal to the upstream water level minus the downstream water level. As seen, subtracting the upstream water level from the downstream water level would typically yield a value of less than 10 ft. Accordingly, to be conservative, a load equivalent to 15 ft of differential hydrostatic head was placed on Lock 27, with the upstream water level chosen to be the mean value of the plot seen below, which was approximately 47 ft.

Figure 15. Selection of water levels for Lock 27.

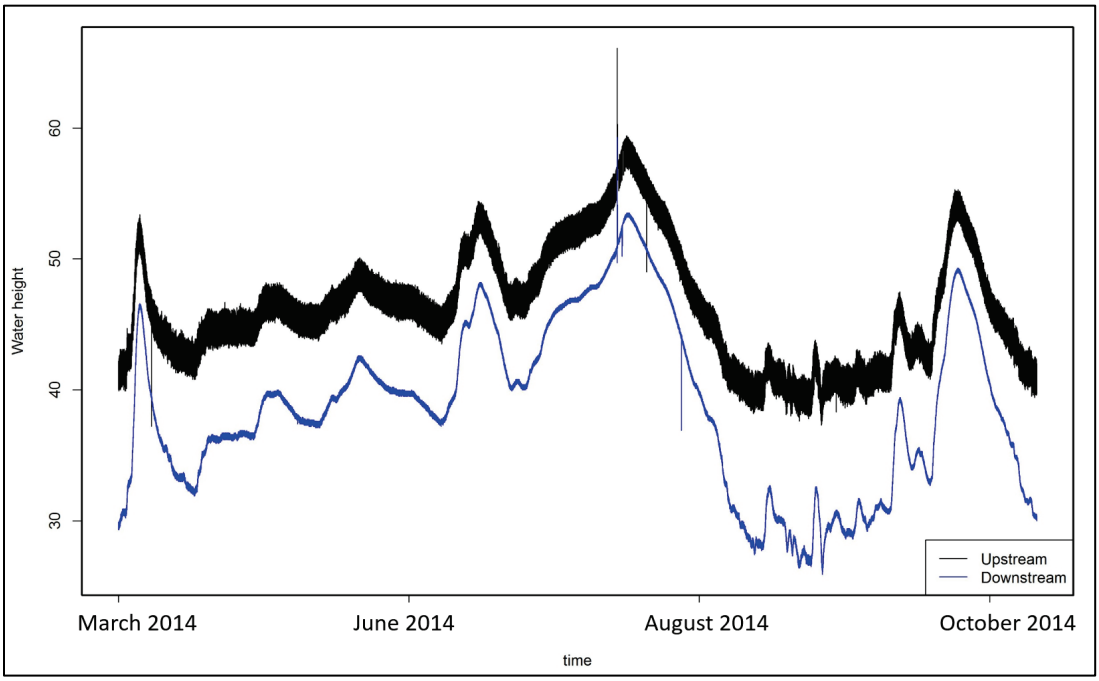

3.3 Contact block modeling

In previous modeling efforts (Eick 2018), the quoin area of the lock gate was greatly simplified by using a simple pin boundary condition that was applied to a line of nodes along the entire height of the quoin. This simplification was reasonable because, for those analyses, stress values immediately next to the quoin were not of interest to the study. However, for the research presented herein, the magnitude of stress immediately next to the quoin is of critical importance. To model the quoin area of the miter gate as accurately as possible, separate quoin block and wall parts were created in Abaqus by using 3D solid elements and accurately modeling them to reflect the convex and concave surfaces, as detailed in the structural drawings. Examples of these parts are shown in Figure 16,

where (a) shows a plan view of the concave wall piece, convex contact block piece, and quoin area of the gate, showing how these piece are situated in the Abaqus assembly. Discontinuous blocks were also modeled with 3D solid elements and the same cross-sectional geometry as the continuous blocks. The discontinuous blocks were also tied to the end of the gate and placed such that they span the width of the girder's flange plus an overhang of 2 in. on both sides of the flange. One such discontinuous block is shown in Figure 17. The Greenup gate is unusual compared to the others because it has intermediate thrust plates in the quoin region between girders, and these plates were found to transfer significant load into the lock wall. Thus, for Greenup, the discontinuous block pieces were placed at the ends of every girder, as well as at every intermediate thrust plate.

Then, to accurately model the intended thrusting behavior of the quoin block region of the lock gate, contact definitions were used between the wall piece and the contact block, as shown in Figure 16a. Convergence issues are common when modeling complicated contact problems in Abaqus. When using surface-to-surface contact in Abaqus, master surface and slave surface must be defined. For this study, it was helpful to define the surface on the contact block to be the master surface while the surface on the wall would then be the slave surface. Additionally, the contact behavior in the normal and tangential directions need to be defined. For the contact normal behavior, the behavior was defined to be "hard" contact, allowing any pressure to be transmitted between contact surfaces when they are in contact, but the surfaces were allowed to separate after contact. For tangential behavior, a "rough" surface was assumed such that no frictional sliding was permitted between surfaces that are in contact. Contact constraints were enforced by means of the "Direct method," which strictly enforces the specified contact behavior without approximation. To facilitate convergence, it was helpful to utilize the node-to-surface discretization method, which interpolates contact conditions from a group of master nodes to a point on the master surface that is projected from the slave node. In addition, small sliding was used for contact tracking, which is distinctly different from the tangential contact definition. See the Abaqus documentation (Dassault Systems 2017), which assumes that the relative motion of contact surface is small. Finally, convergence was facilitated by forcing the solver to adjust a line of nodes on the wall piece to be in perfect contact at the start of the analysis. For more information on the specifics of defining contact in Abaqus, the reader is directed to review the software's documentation (Dassault Systems 2017).

Figure 16. (a) Plan view of concave wall part, convex quoin block part, and gate, showing how the block and wall quoin are situated and modeled in the Abaqus model; (b) elevation view of wall part, quoin block part, and gate.

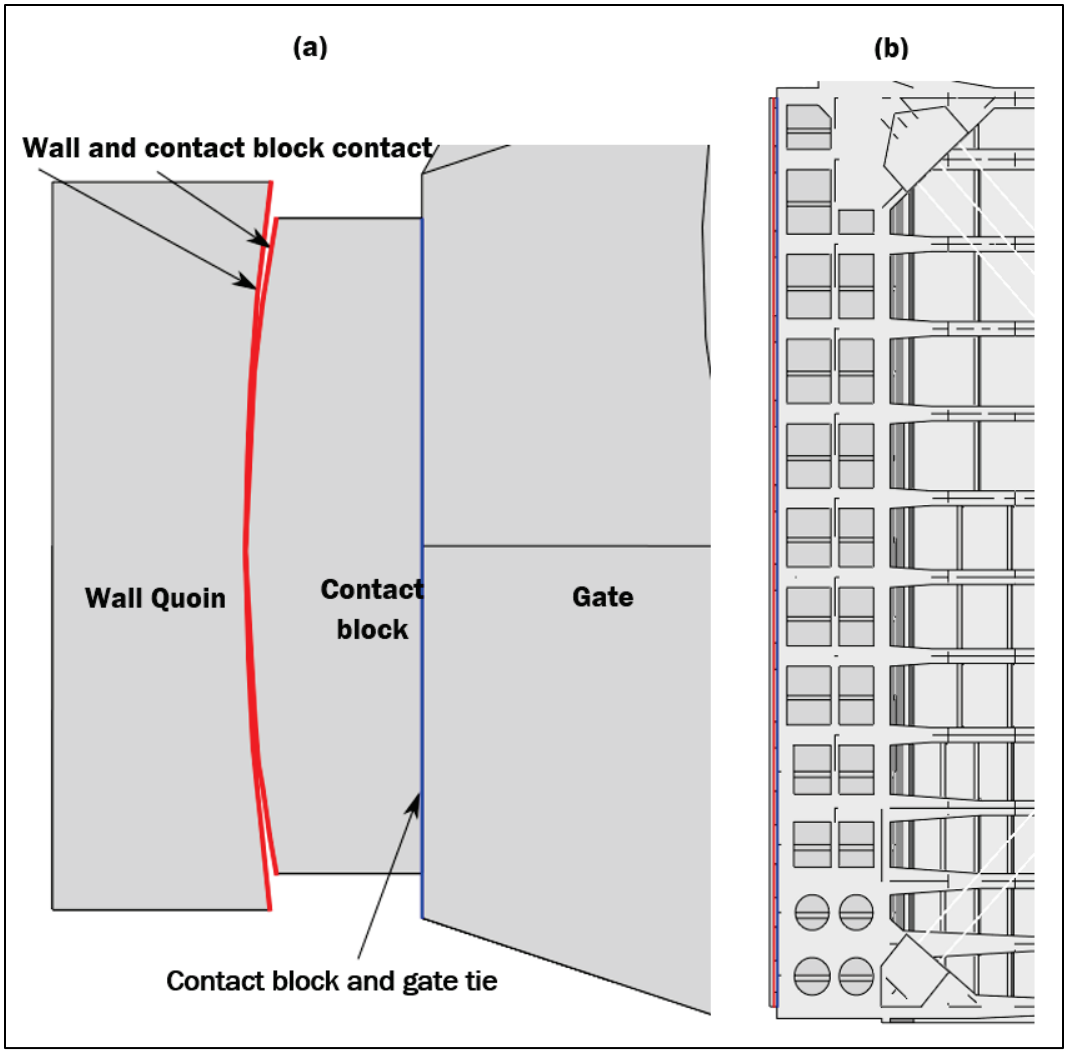

Figure 17. Discontinuous block, showing the 2 in. overhang and the coincidence with the horizontal girder.

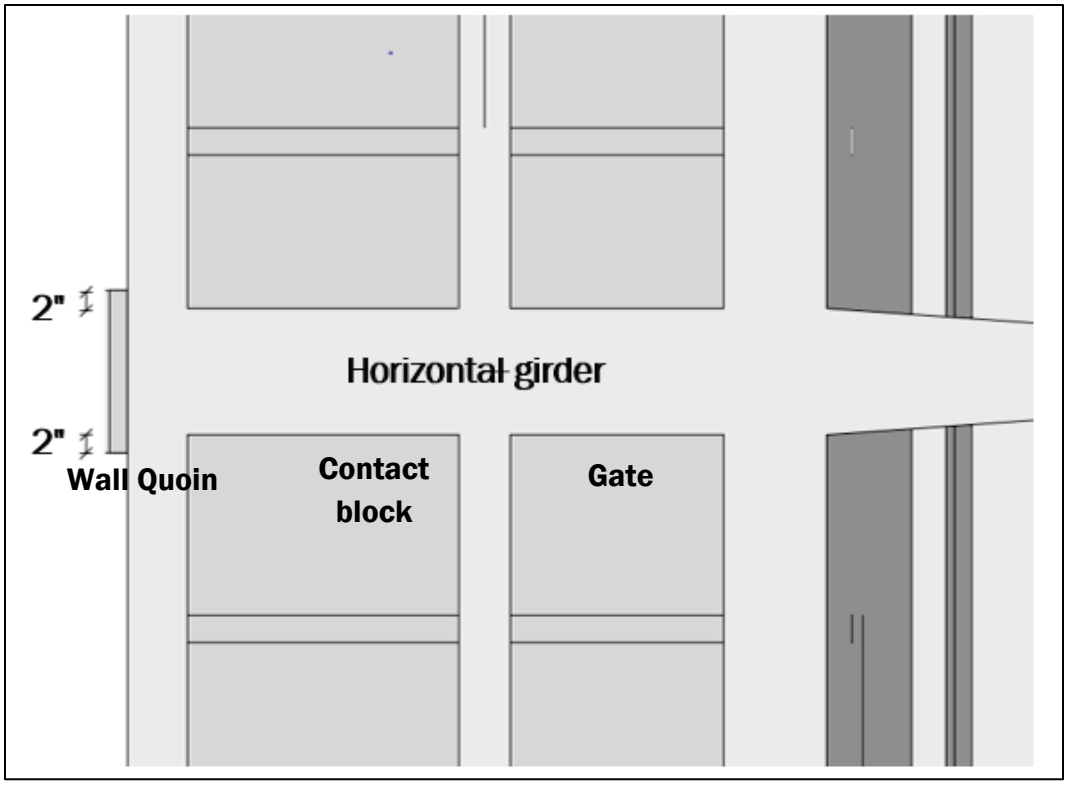

3.4 Boundary conditions

Contact block and gate tie

For these analyses, in addition to the contact described above, a set of basic boundary conditions was applied to each lock gate. Overviews of the boundary conditions are shown in the elevation view in Figure 18 and again in the plan view in Figure 19.The pintle and gudgeon anchors of each lock gate were pinned, and a roller-type support was applied to a line of nodes along the entire height of the location corresponding to the miter block. To more accurately simulate the pintle region, a small area of nodes in the pintle region was constrained to the location corresponding to the pintle-ball center point using a beam-type multi-point constraint (MPC). To accurately simulate the anchorage links, the links were oriented at the appropriate angles to represent one primary and one secondary anchorage typical of miter gates. Anchorage links do not have a constant cross section. To approximate this, a constant cross-sectional area was used in the model such that the modeled anchorage would have an axial stiffness similar to the average stiffness of the physical anchorage link. The anchorage links were constrained at one end to a beam representing the gudgeon pin using an MPC-pin constraint (which ties translational, but not rotational, degrees of freedom). A pinned boundary condition was

then applied to the opposite end of the anchorage links. The gudgeon pin itself was modeled using a beam spanning between the top girder and the gudgeon hood; the ends of the gudgeon pin were constrained to appropriately sized holes in the top girder and gudgeon hood by using a beam-type MPC.

Figure 18. Elevation view of gate, highlighting boundary conditions.

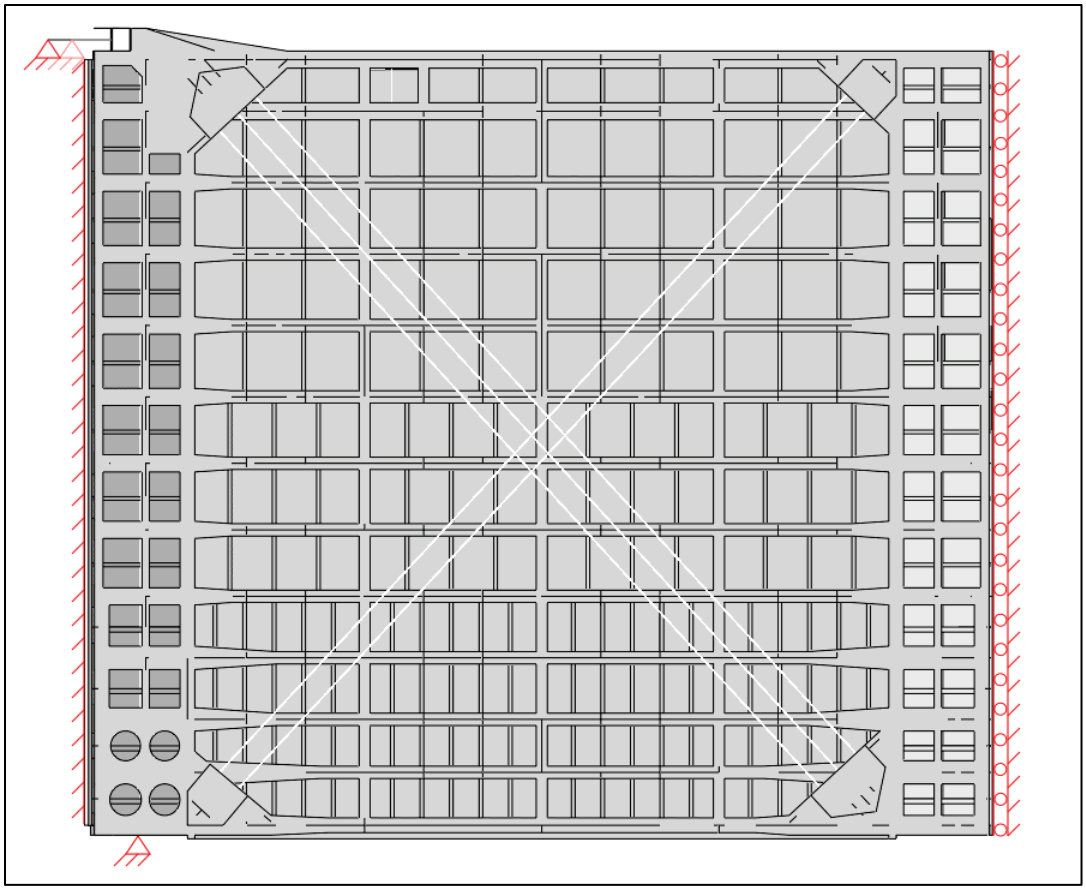

Figure 19. Plan view of gate highlighting boundary conditions.

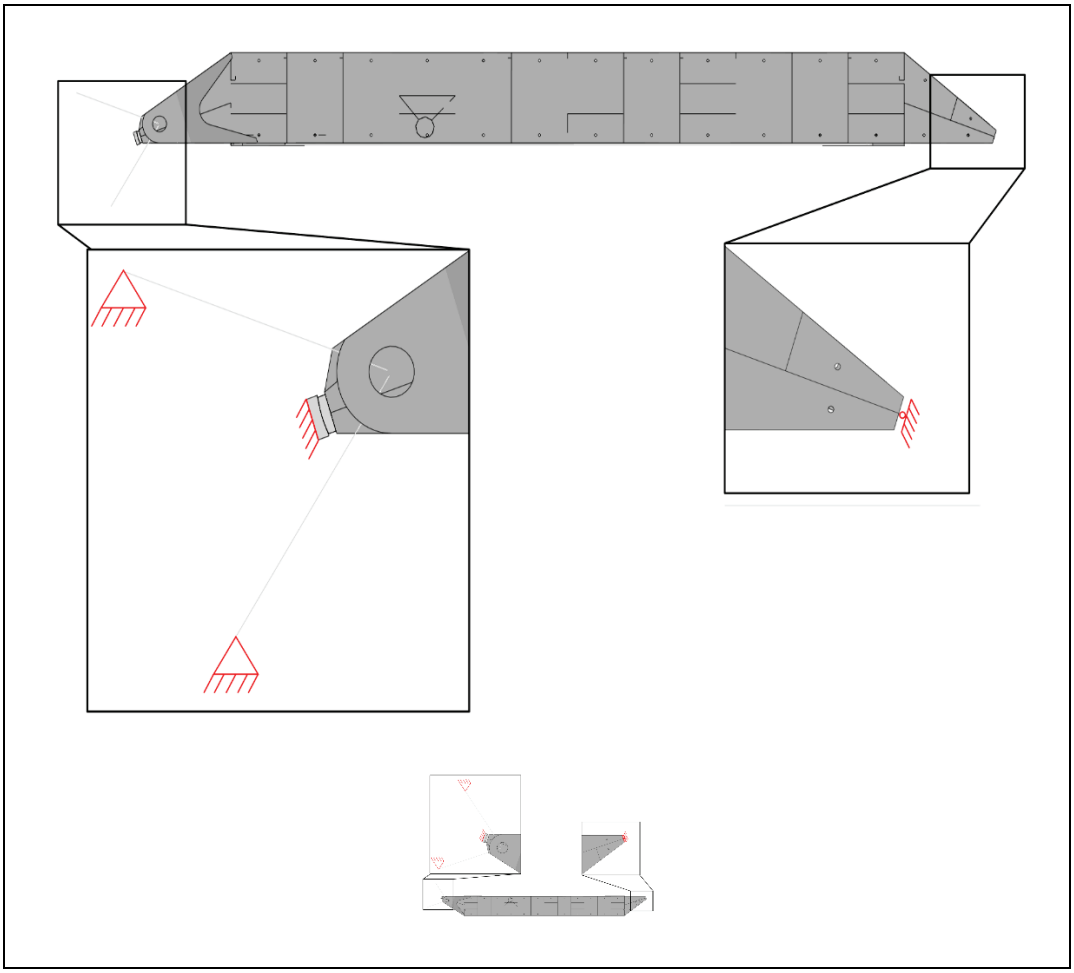

3.5 Damage tolerance and quoin gaps

To test the damage tolerance of discontinuous quoin blocks, analyses were also run that considered gaps in the contact surface in the quoin block. Two gap scenarios were considered—a gap near the bottom of the gate (herein called the "low gap"), and a gap near the typical high water level for the gate (herein called the "mid gap"). Both gaps were 12 ft in length, with a maximum depth of ¼ in. The gap near the bottom of the gate was at maximum depth at the bottom of the quoin block, and tapered to no gap 12 ft above. The gap at the high water level had maximum depth at the high water mark and tapered to no gap at 6 ft above and below the high water mark. The gaps were modeled by altering the geometry in the contact blocks themselves. Representative geometry of the gaps is shown in Figure 20. The high water levels used for each mid-gap scenario are shown in Table 3.

Figure 20. Representative geometry for (a) low gap and (b) mid gap.

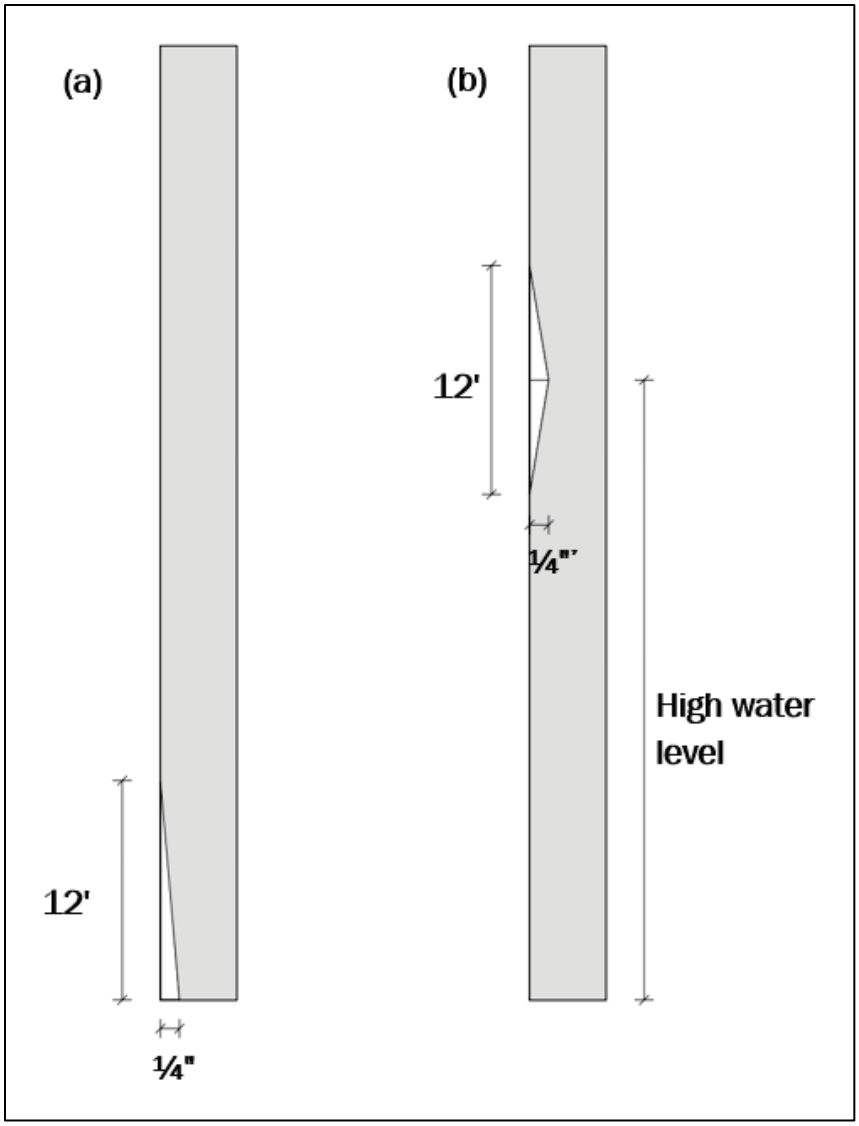

Table 3. High water levels for mid-gap scenario locations.

Gate	High Water Level
Lockport	48'-4"
Terry	27'-6"
Racine	38'-8"
Greenup	45'-0"
Cannelton	40'-0"
Lock 27	40'-0"

4 Results

This section provides the relevant results for the discontinuous quoin block study. First, an explanation of where results were investigated is given, as will an explanation as to why this was reasonable. Then, results are given for each model, with each gate having its own subsection.

4.1 Description of results investigated

During the course of investigating, it became apparent that the change in stress between a lock gate with discontinuous quoin blocks and one with continuous quoin blocks was largely confined to the area of the gate immediately next to the quoin block itself. This finding is demonstrated in Figure 21, which is a contour plot showing the change in the Lock 27 miter gate between the scenario with a continuous block and the scenario with a discontinuous block. The contour plot is set up such that dark blue/black represents a very negative change, while bright red/white represents a very positive change. Zero change is effectively represented by green. As seen in the contour plot, changes in stress between the two quoin block cases are largely confined to the area immediately next to the quoin of the gate. While the contour plot is shown here for only one lock gate (Lock 27), the results for all analyses were similar. Because of the localized nature of the change in stress, only stress results in the area of the gates immediately next to the quoin was investigated. Further, due to the typical gradient in hydrostatic load on the gate (refer to Figure 14), it is known that the magnitude of stress at the top of the gate is largely inconsequential; therefore, only stress in girders in the bottom half of the gate was investigated.

Figure 21. Contour plot showing change in stress between continuous and discontinuous quoin blocks.

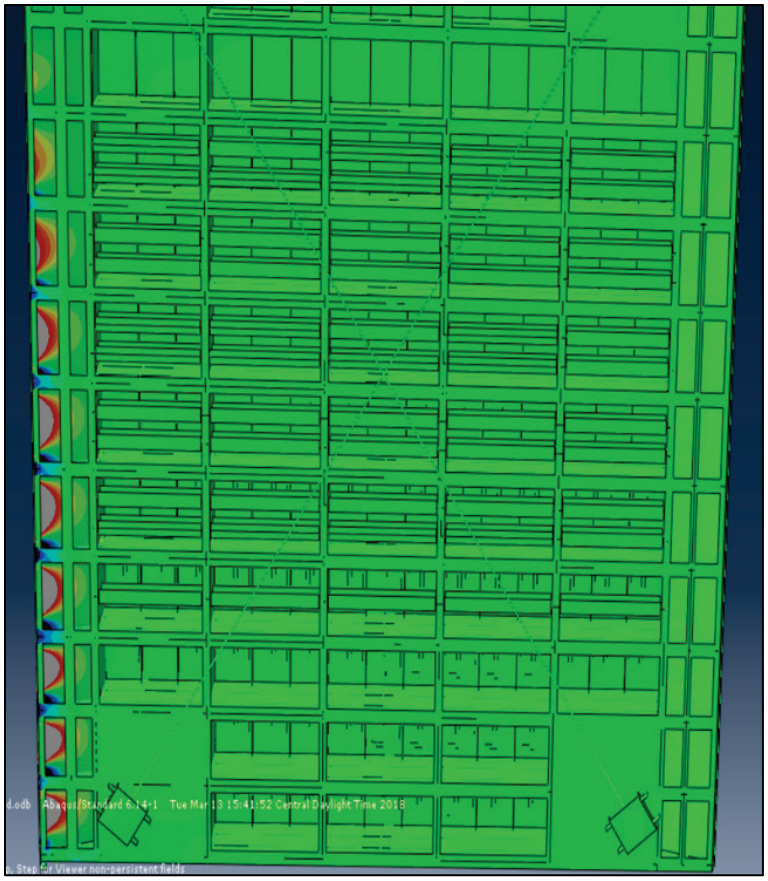

It would be inefficient to show plots and tabular data for all components of stress for all locations on the gates, so for this study it is deemed sufficient to simply report the von Mises stress invariant for each analysis. The von Mises stress is a scalar combination of all the stress components at a location, the value of which is frequently used as a yield criterion for ductile materials; for instance, if the von Mises stress is greater than the material's yield strength, the material is considered to have yielded.

The results that follow are tabulated for girders in the bottom half of the gate for the region immediately next to the quoin. The von Mises stress is recorded for six regions of interest on each girder: upstream flange, downstream flange, web, end plate, upper thrust diaphragm, and lower thrust diaphragm. The regions of interest are shown as areas A–E in Figure 22 and Figure 23, with their designation explained in Table 4. In each region, the von Mises stress of every element is investigated and the

maximum is recorded. Therefore, for each girder investigated, there will be 18 stress values (three damage scenarios for six locations per girder).

Figure 22. Upstream elevation and details showing results locations.

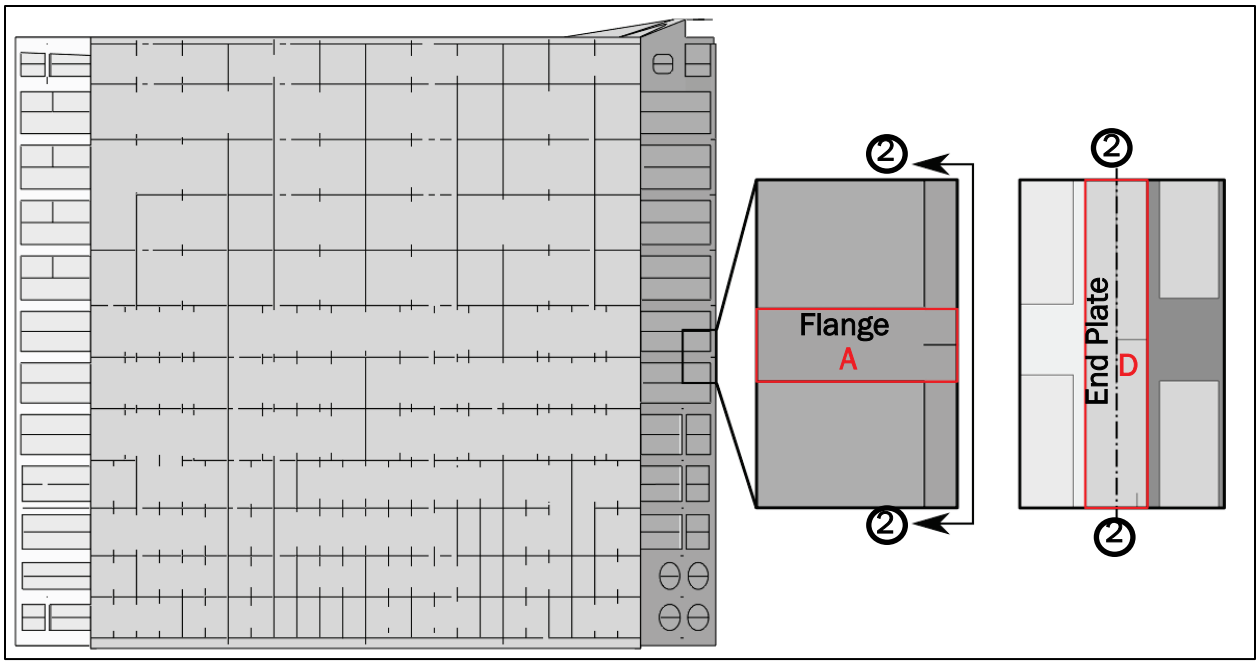

Figure 23. Downstream elevation and details showing results locations.

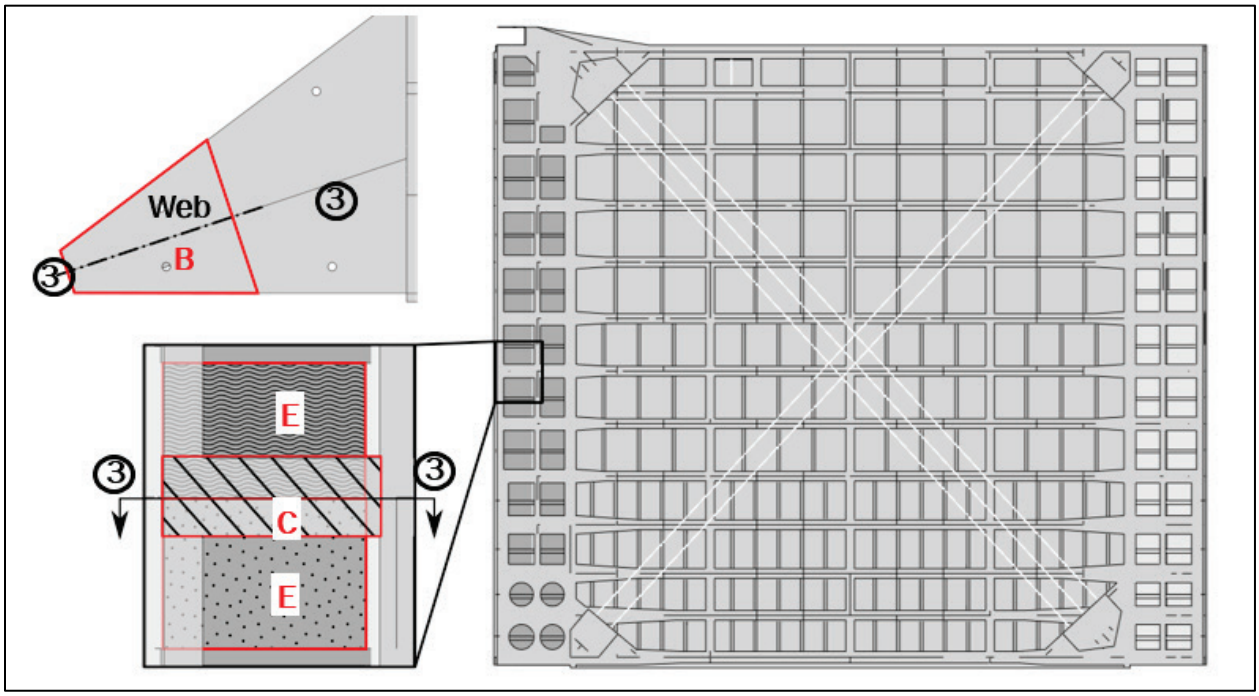

Table 4. Designation and explanation of results locations.

Designation	Description
A	Upstream flange
B	Web
C	Downstream flange
D	End plate
E	Thrust plate

In sections 4.2 to 4.7, results for each lock gate and each damage scenario are presented in figures consisting of a collection of bar graphs, and a representative plot is shown in Figure 24 (note, tabulated values of the results are shown in Appendix A). Each bar graph represents one of the locations described in Table 4, as shown in the label along the *x*-axis. The individual sets of bars represent the girder being reported, as noted in the label on the *y*-axis. Gray bars represent the maximum von Mises stress recorded from the discontinuous quoin analysis while the black bars represent the maximum von Mises stress recorded from the continuous quoin analysis. A dashed vertical line is placed along 50 ksi to mark the typical yield stress of steel for comparison. The plots are laid out to emulate the typical elevation view of a lock gate, since the girder with the highest number is at the bottom and the girder with the lowest number is at the top. As a reference to the gate geometry and the location of the girder numbers, an elevation view taken from the structural drawings is also provided for each gate.

Figure 24. Typical results plots.

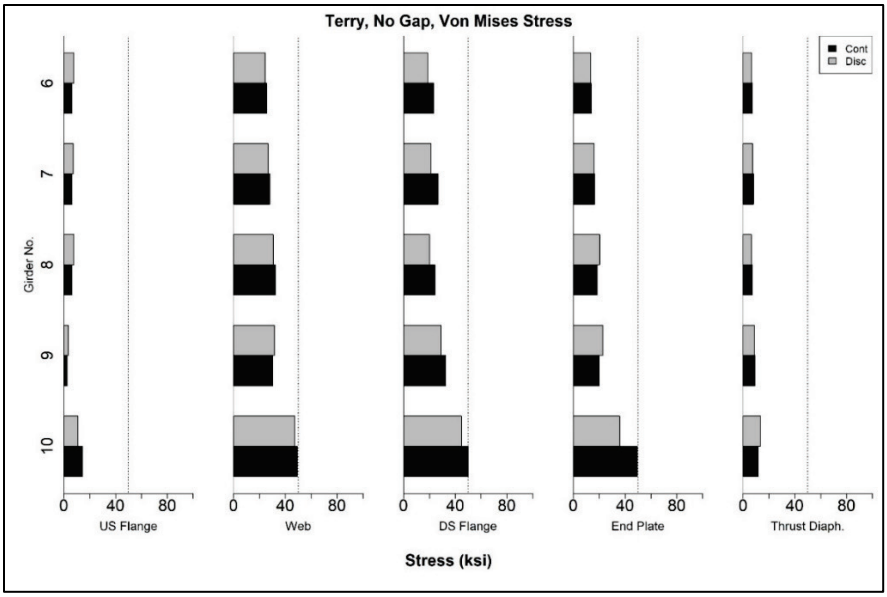

4.2 Lockport

An elevation view of the modeled gate leaf at Lockport is shown in Figure 25. Figure 26 shows the results for the scenario with no gap, Figure 27 shows the results for the scenario with a low gap, and Figure 28 shows the results for the scenario with a mid gap.

Figure 25. Elevation view of Lockport.

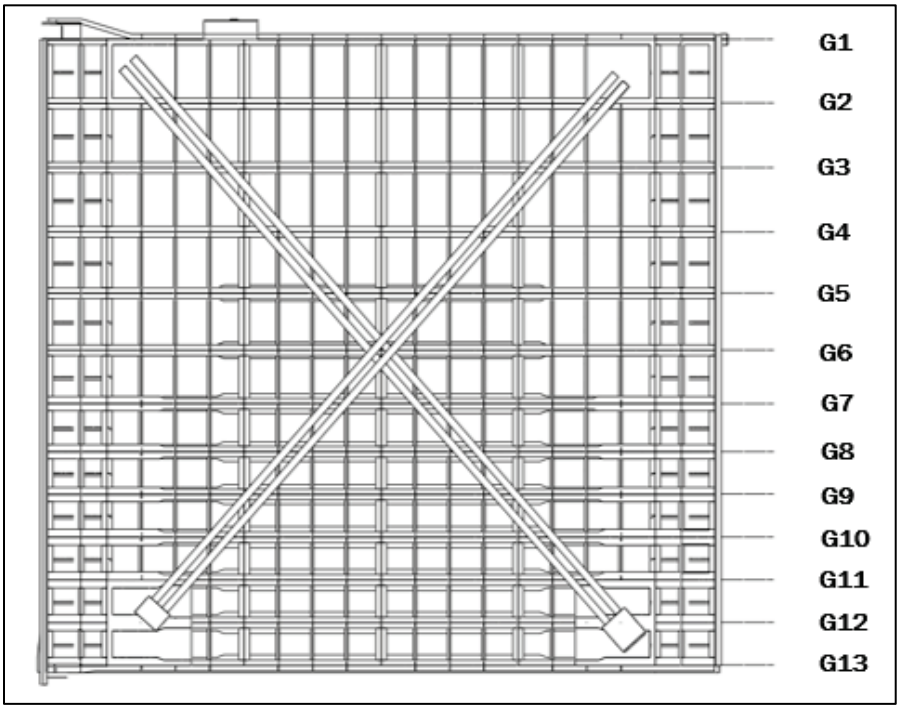

Figure 26. Results for Lockport, no-gap scenario.

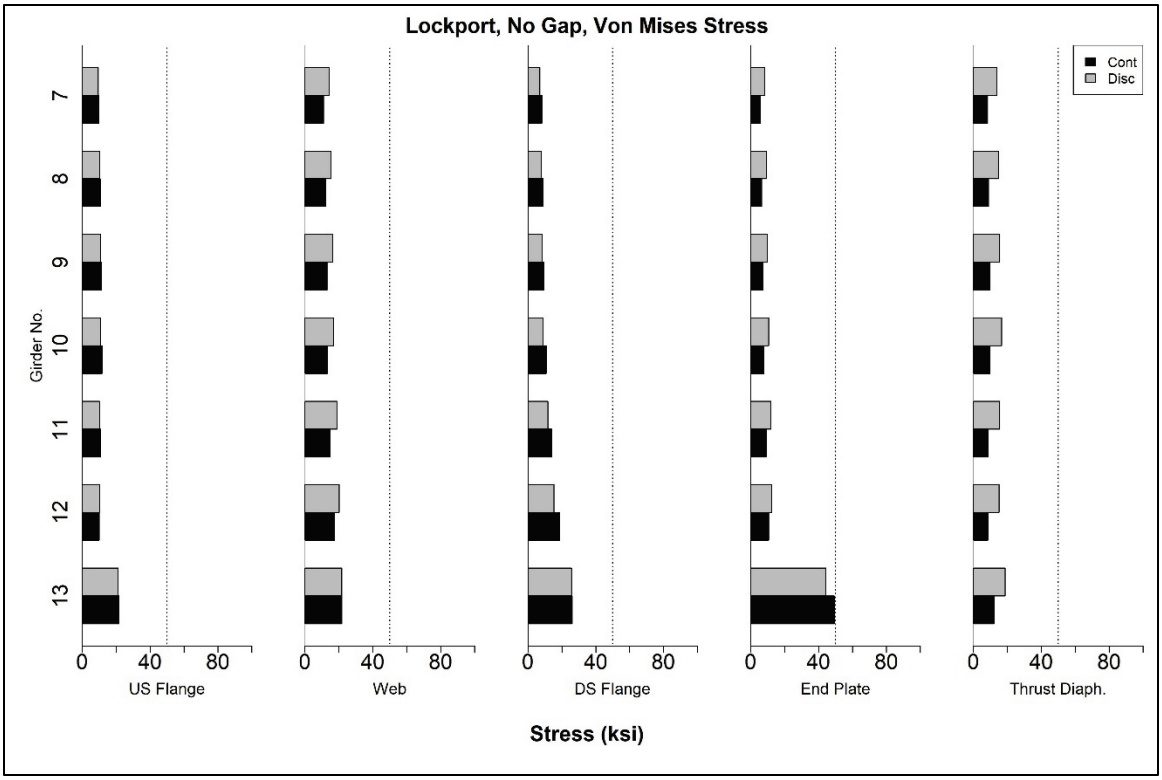

Figure 27. Results for Lockport, low-gap scenario.

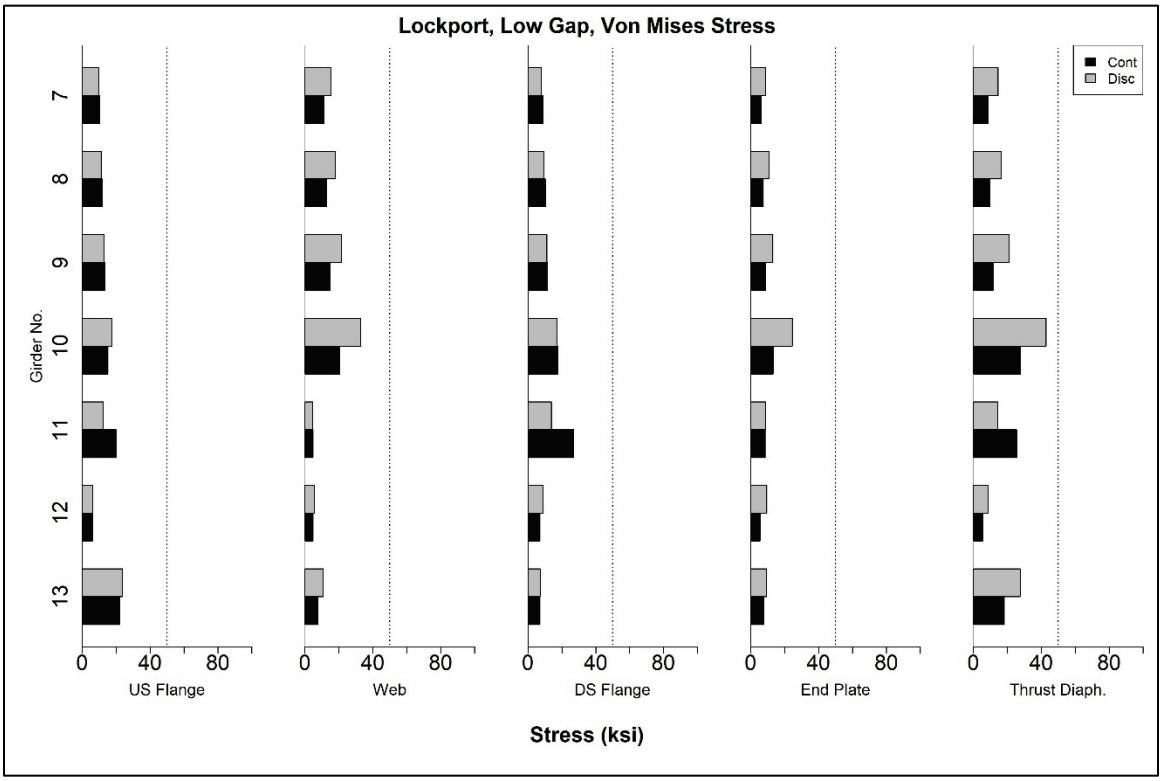

Figure 28. Results for Lockport, mid-gap scenario.

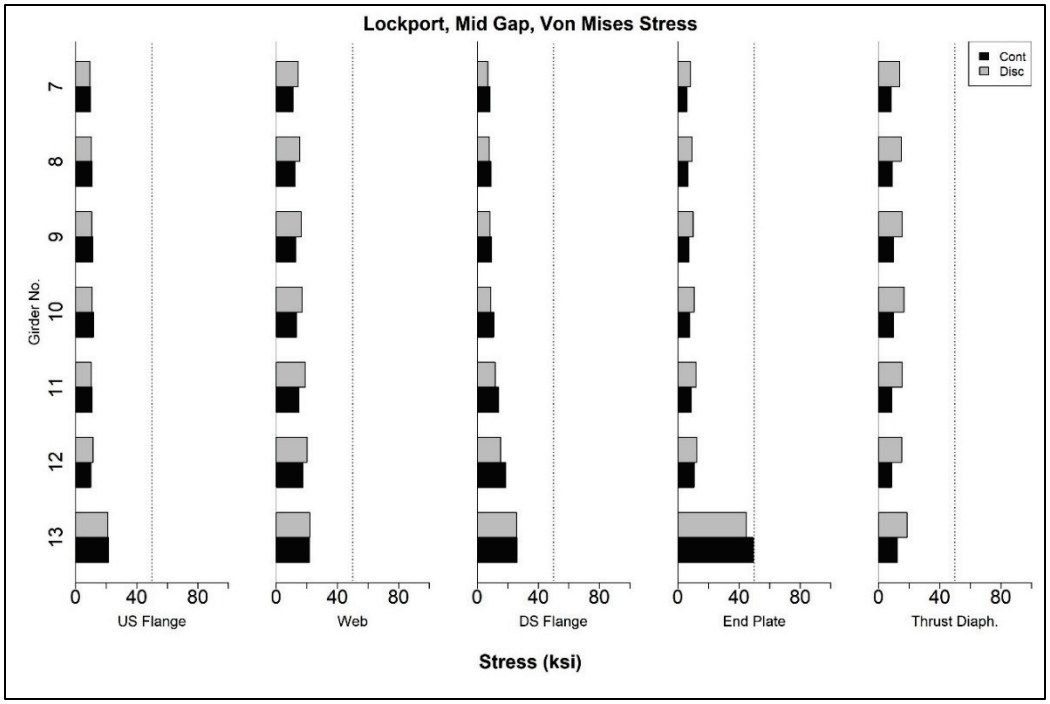

4.3 Terry

An elevation view of the modeled leaf of the David D. Terry Lock and Dam is shown in Figure 29. The results for the no-gap scenario are shown in Figure 30, the results for the low-gap scenario are shown in Figure 31, and results for the mid-gap scenario are shown in Figure 32.

Figure 29. Elevation view of Terry lock gate.

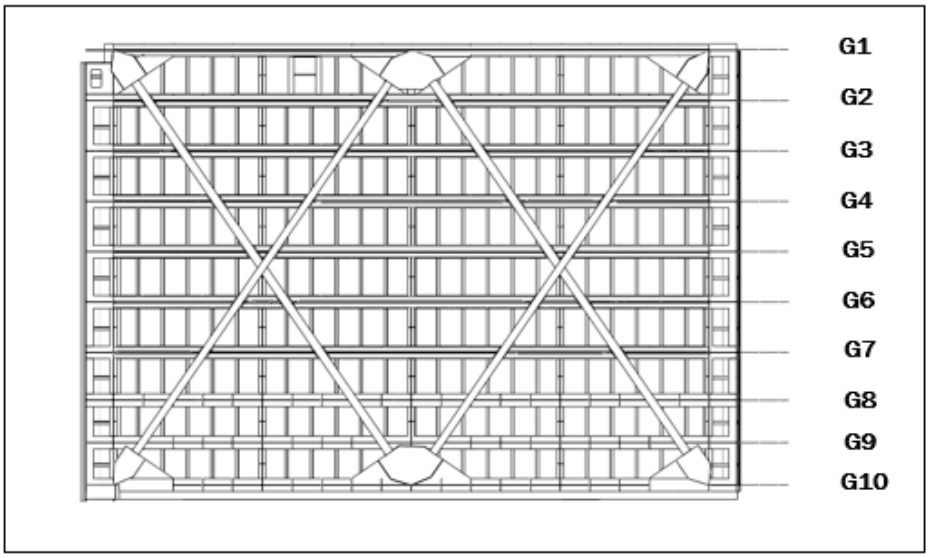

Figure 30. Results for Terry, no-gap scenario.

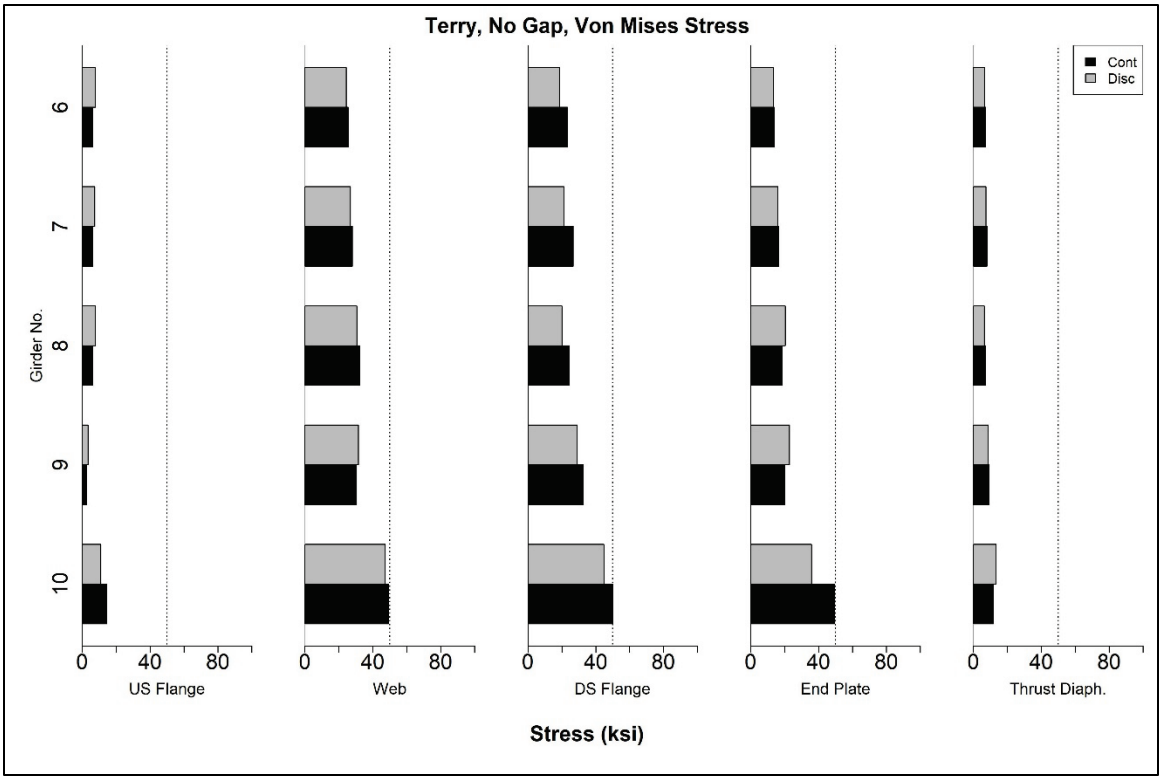

Figure 31. Results for Terry, low-gap scenario.

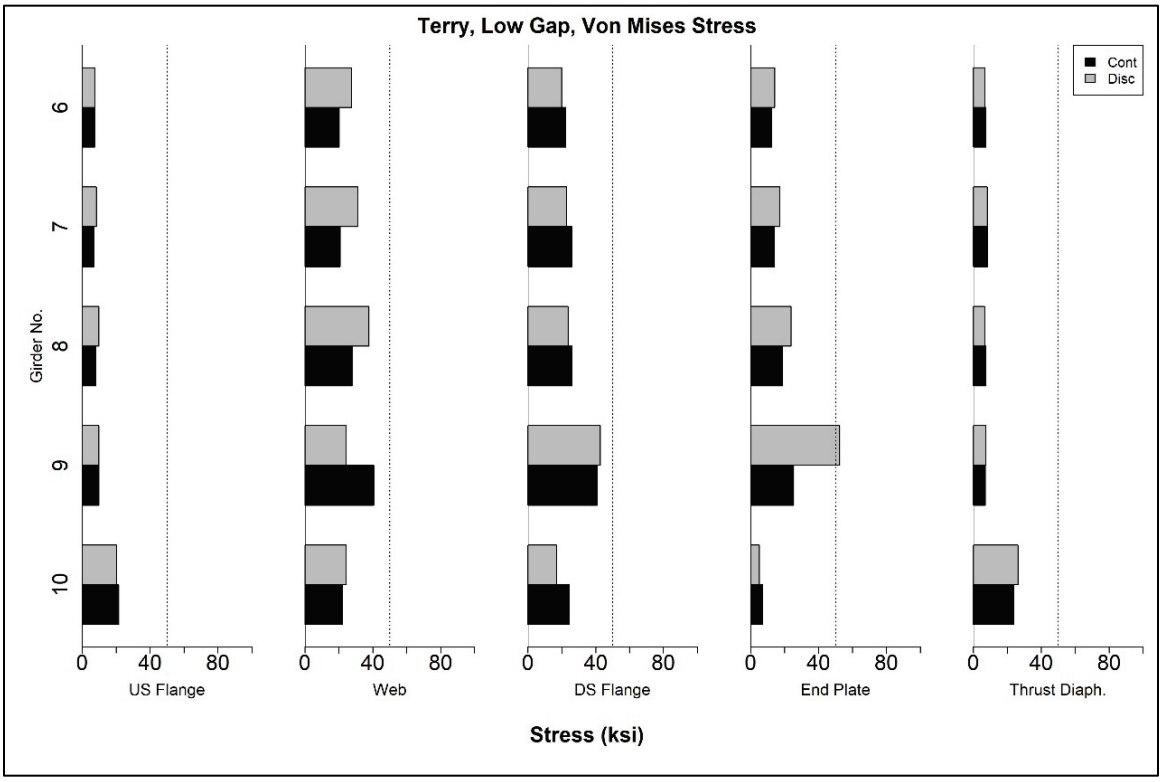

Figure 32. Results for Terry, mid-gap scenario.

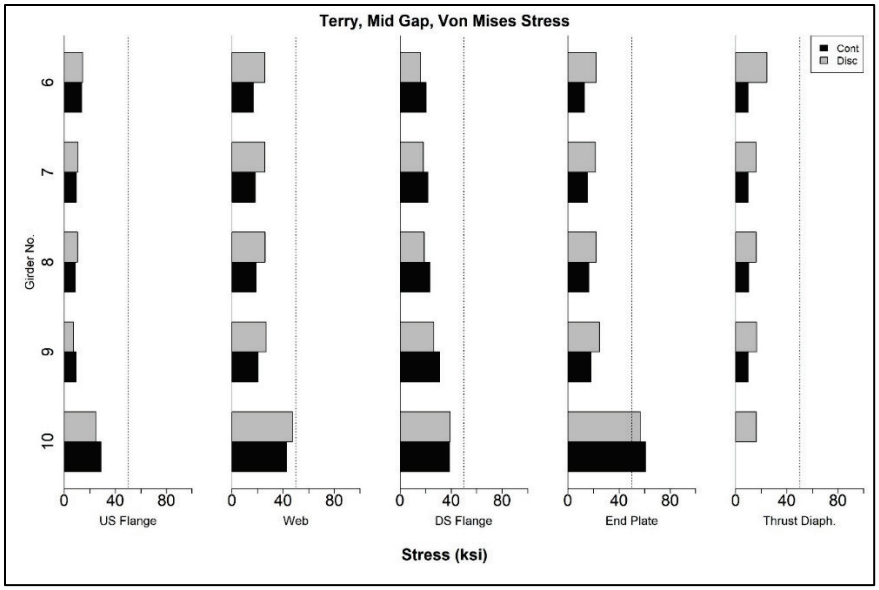

4.4 Racine

An elevation view of the modeled leaf of the Racine Lock and Dam is shown in Figure 33. Figure 34 shows the results for the no-gap scenario, Figure 35 shows the results for the low-gap scenario, and Figure 36 shows results for the mid-gap scenario. Note that results for the web on Girder 13 exceed 100 ksi for both continuous and discontinuous quoin block scenarios. Rather than rescale the plot, it is simply noted that the stress in this region exceeds any reasonable limit criteria.

Figure 33. Elevation view of Racine lock gate.

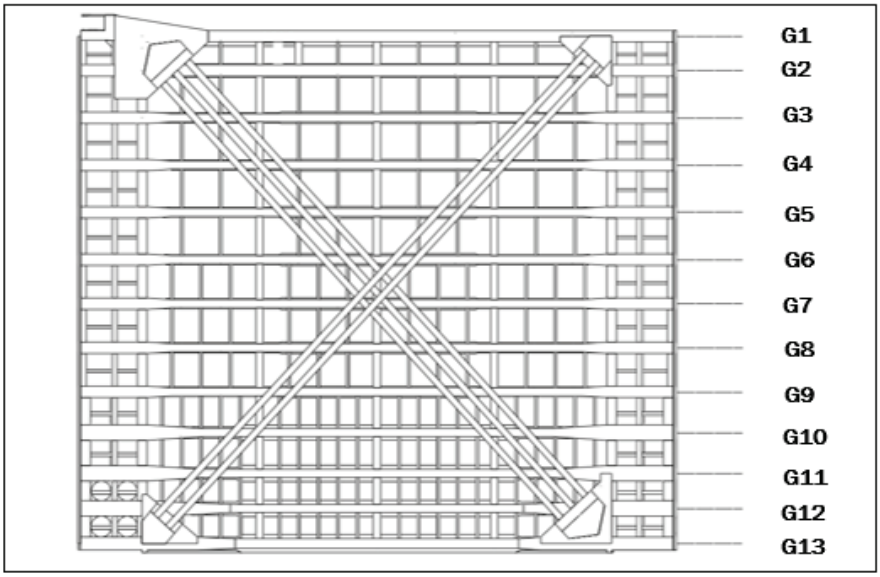

Figure 34. Results for Racine, no-gap scenario.

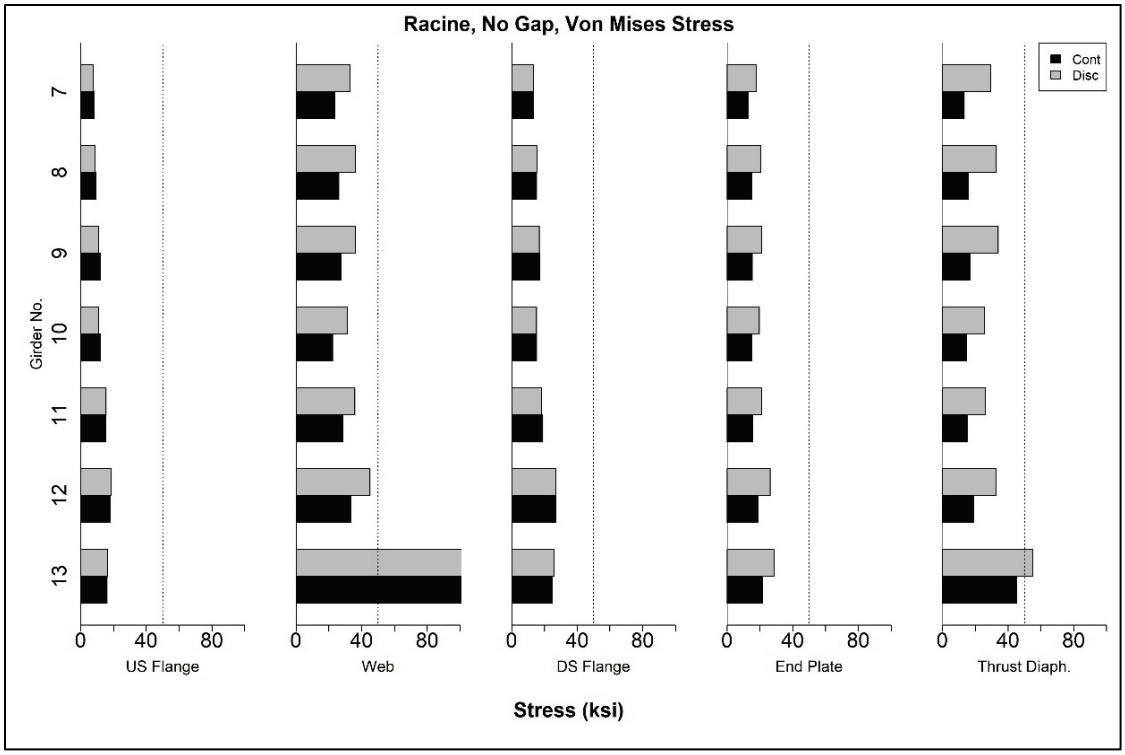

Figure 35. Results for Racine, low-gap scenario.

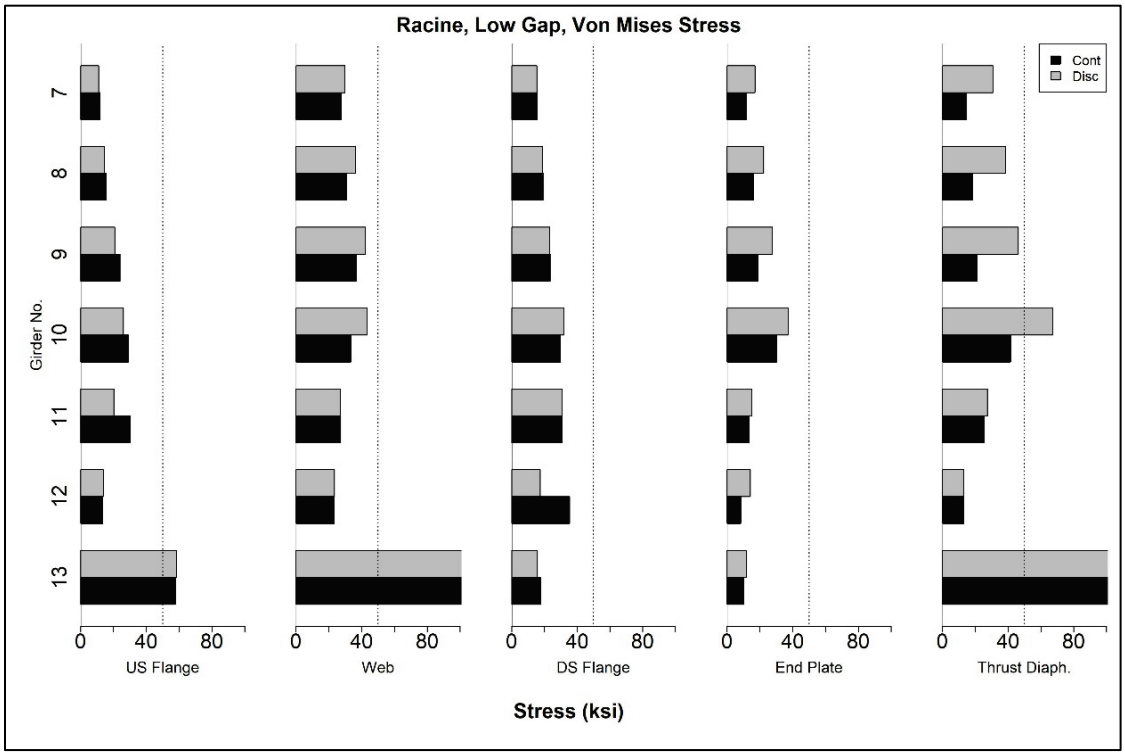

Figure 36. Results for Racine, mid-gap scenario.

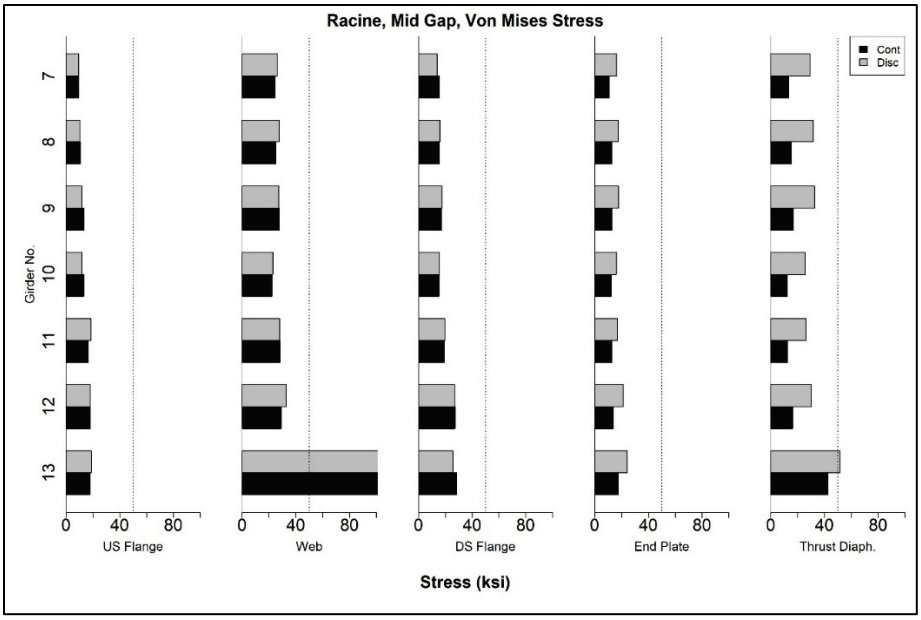

4.5 Cannelton

An elevation view of the modeled leaf of the Cannelton Lock and Dam is provided in Figure 37. The results for the no-gap scenario are provided in Figure 38, while the results for the low-gap scenario are shown in Figure 39, and results for the mid-gap scenario are shown in Figure 40.

Figure 37. Elevation view of Cannelton lock gate.

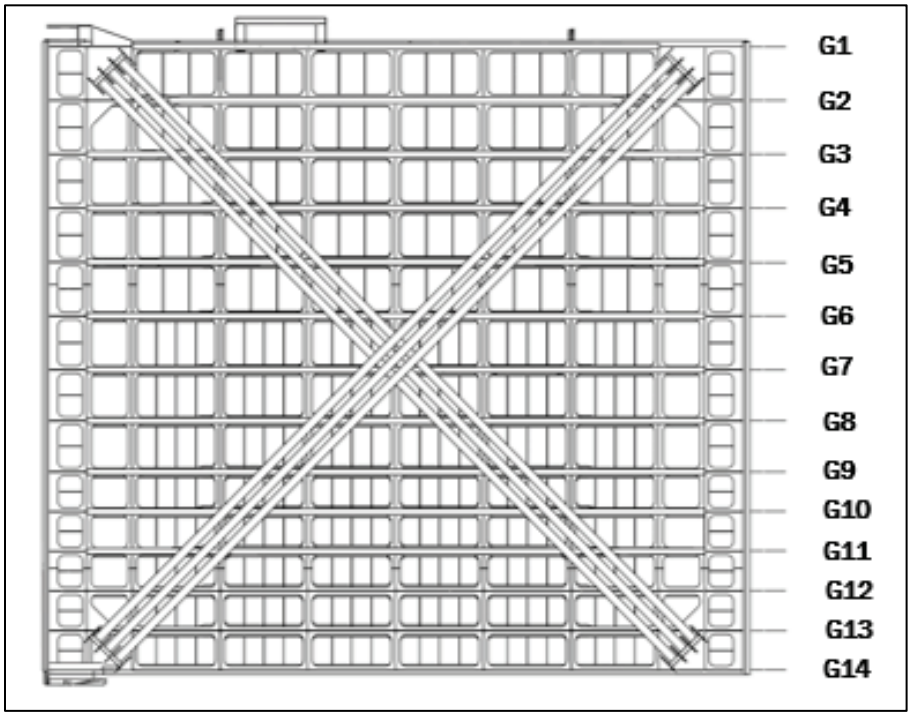

Figure 38. Results for Cannelton, no-gap scenario.

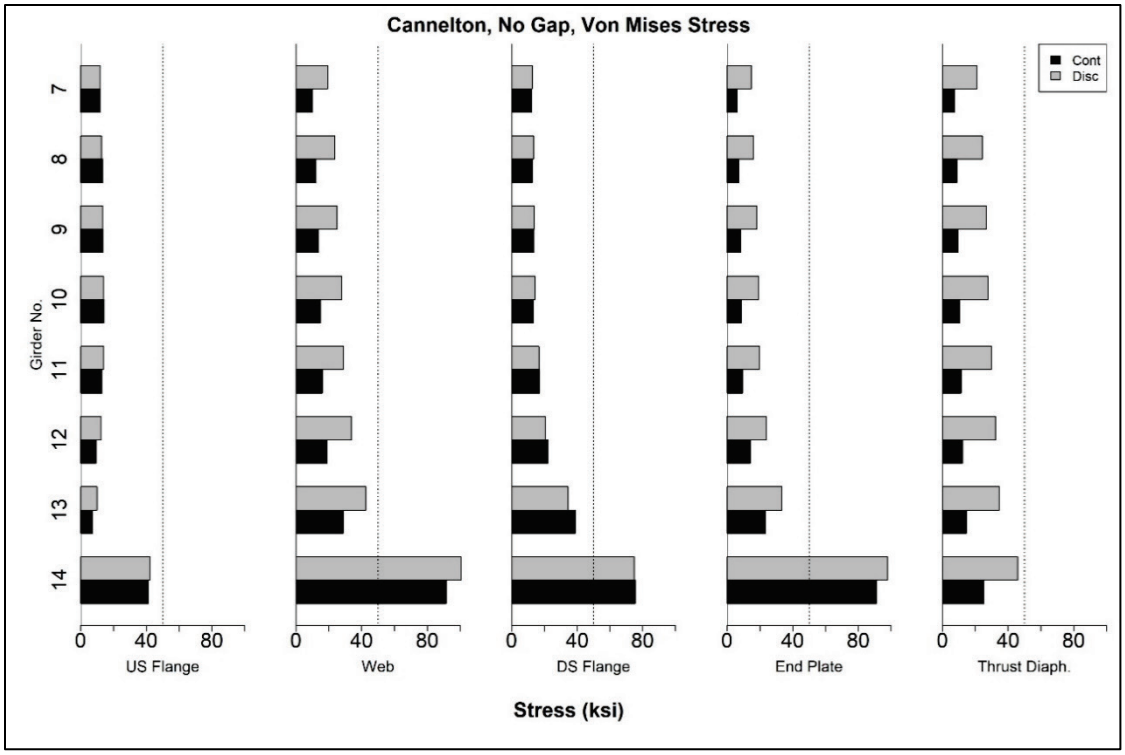

Figure 39. Results for Cannelton, low-gap scenario.

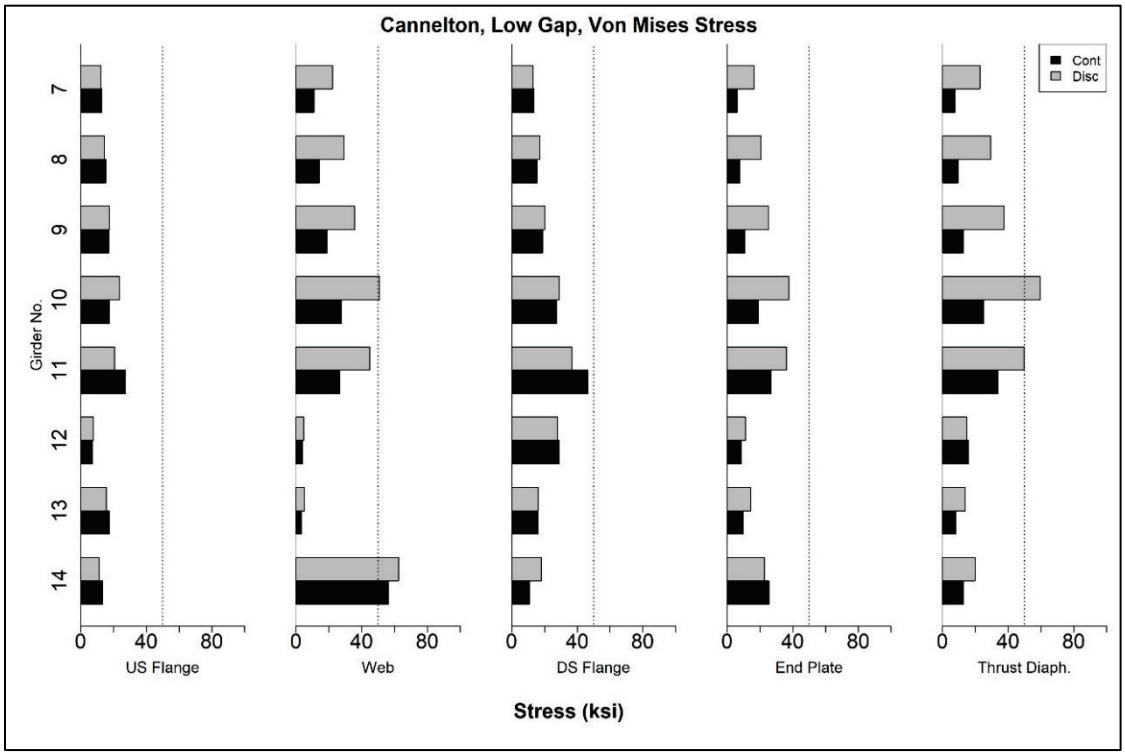

Figure 40. Results for Cannelton, mid-gap scenario.

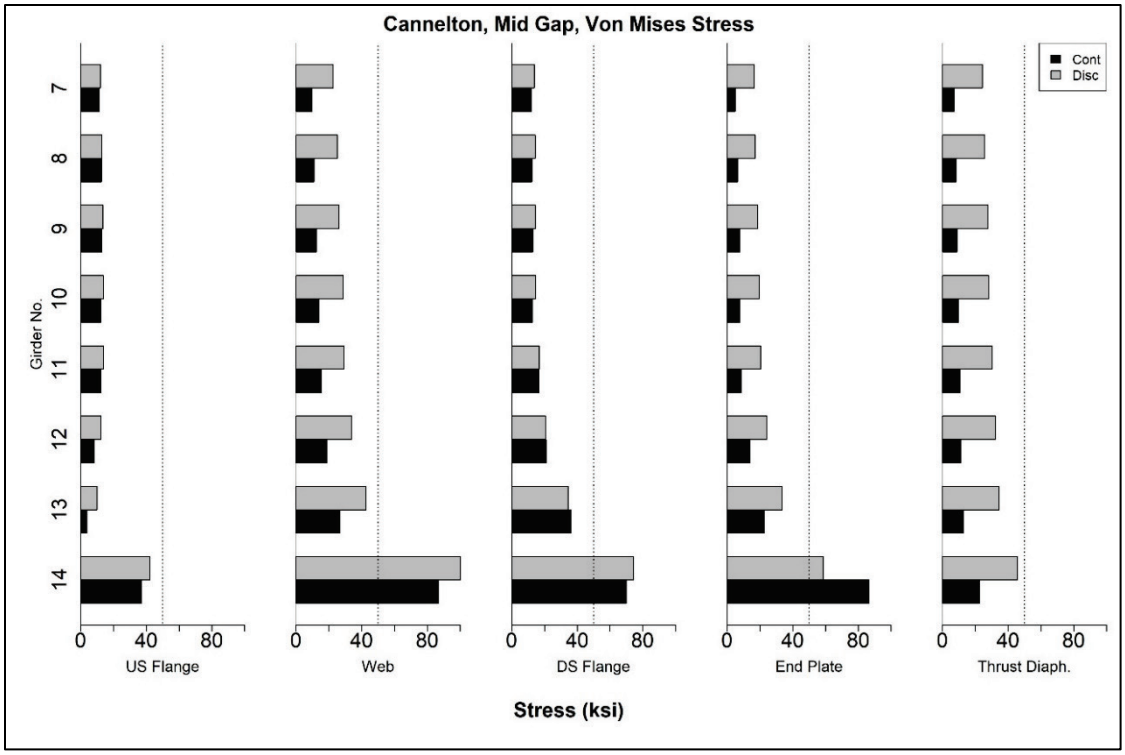

4.6 Greenup

An elevation view of the modeled leaf of the Greenup Lock and Dam site is provided in Figure 41. Results for the no-gap scenario are provided in Figure 42 while results for the low-gap scenario are shown in Figure 43, and results for the mid-gap scenario are shown in Figure 44.

Figure 41. Elevation view of Greenup lock gate.

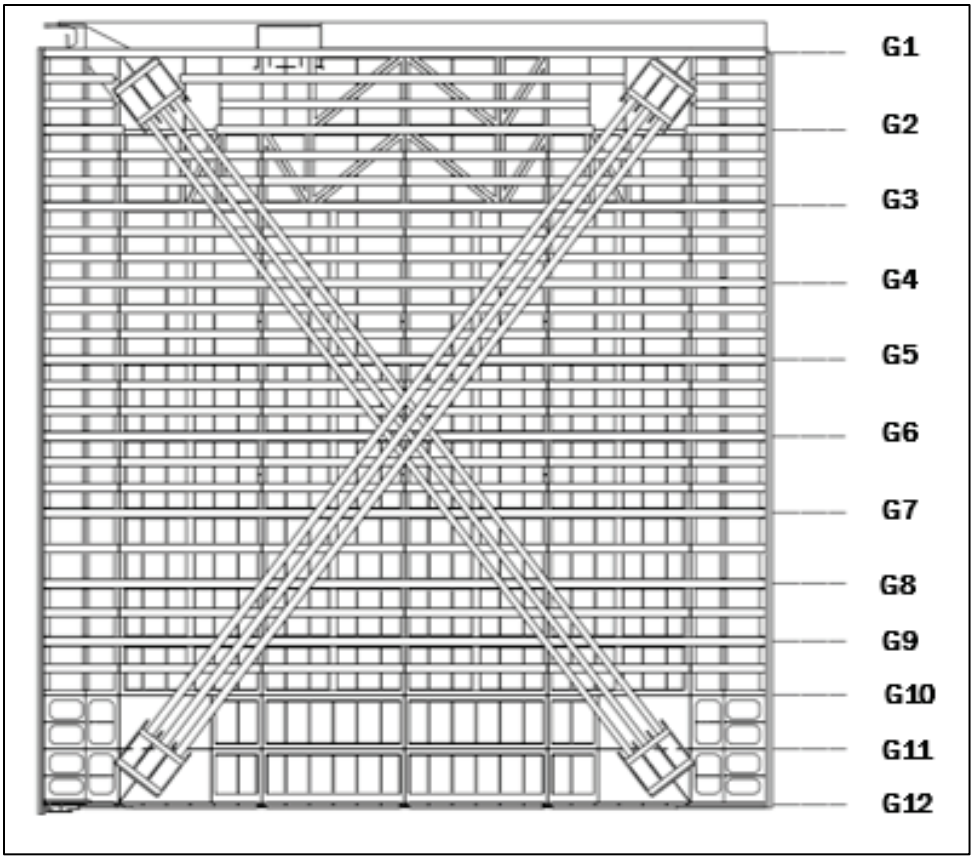

Figure 42. Results for Greenup, no-gap scenario.

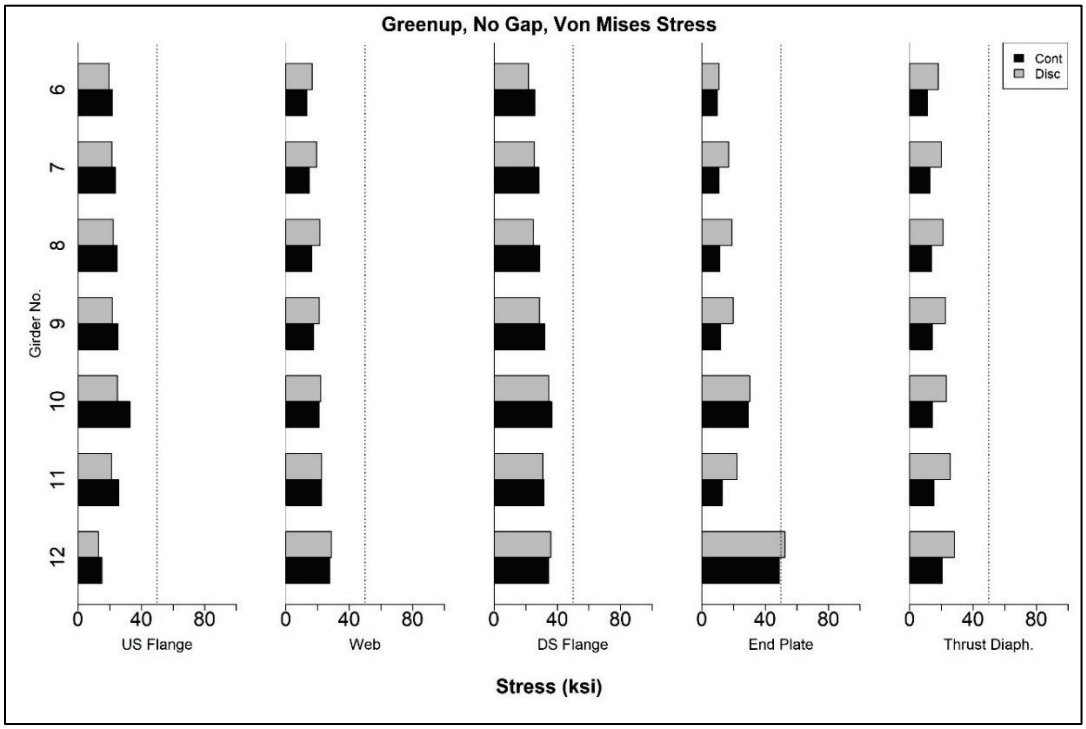

Figure 43. Results for Greenup, low-gap scenario.

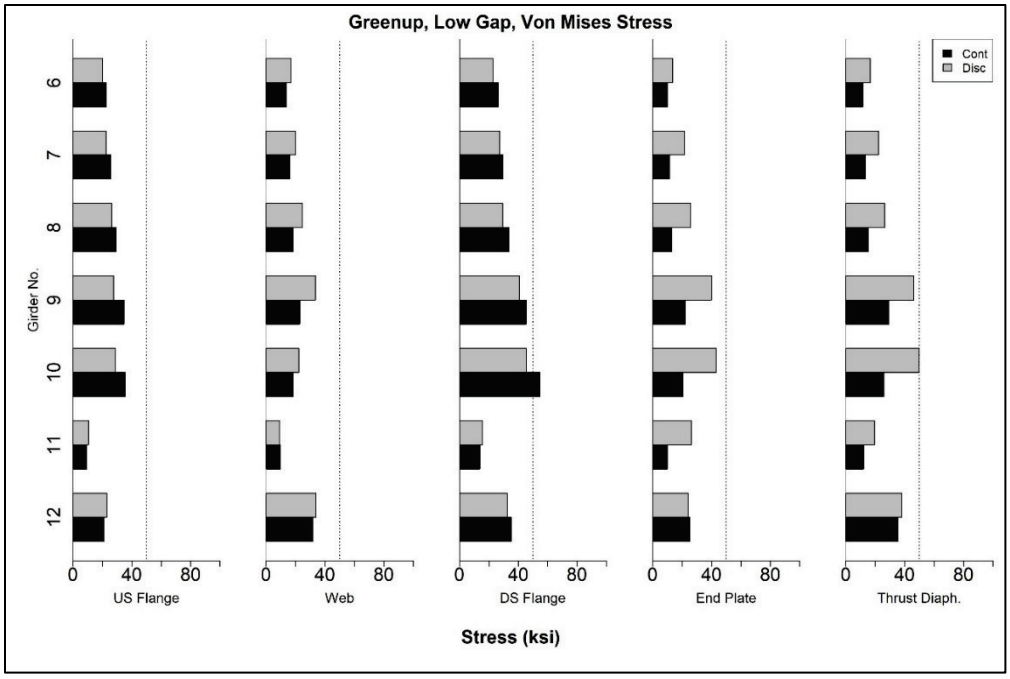

Figure 44. Results for Greenup, mid-gap scenario.

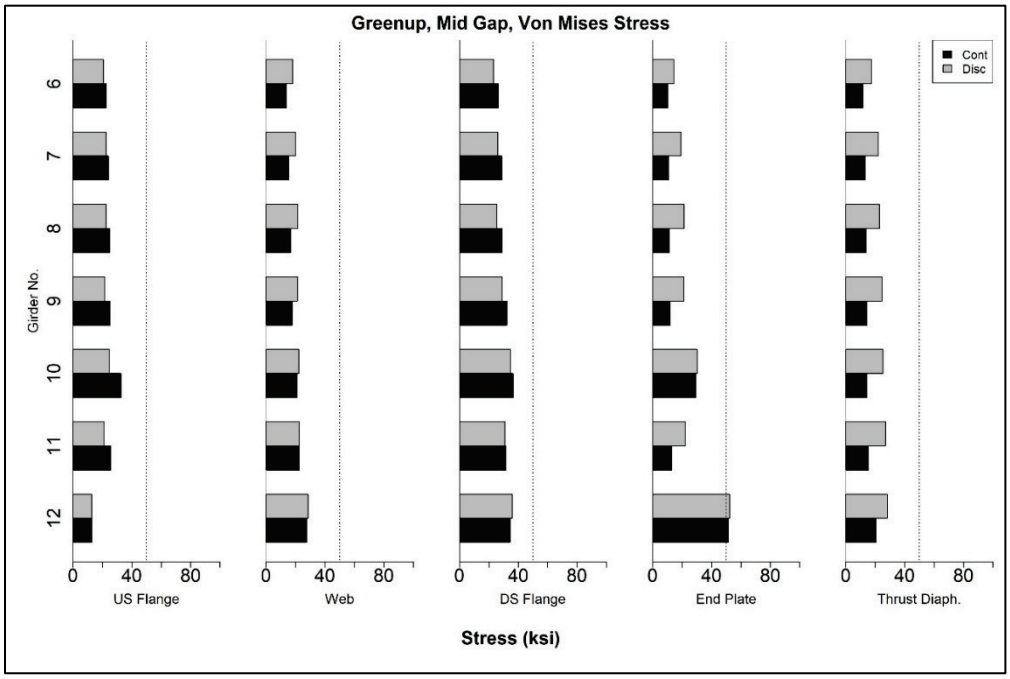

4.7 Lock 27

An elevation view of the modeled leaf for the Lock 27 site is provided in Figure 45. Results for the no-gap scenario are provided in Figure 46 while results for the low-gap scenario are shown in Figure 47, and the mid-gap

scenario results are shown in Figure 48. Similar to the results presented for Racine, rather than rescale plots to accommodate stresses that exceed 100 ksi (e.g., the web of girder 13 for the low-gap scenario), it is simply noted that stress in these regions greatly exceeds any reasonable limit criteria.

Figure 45. Elevation view of Lock 27 lock gate.

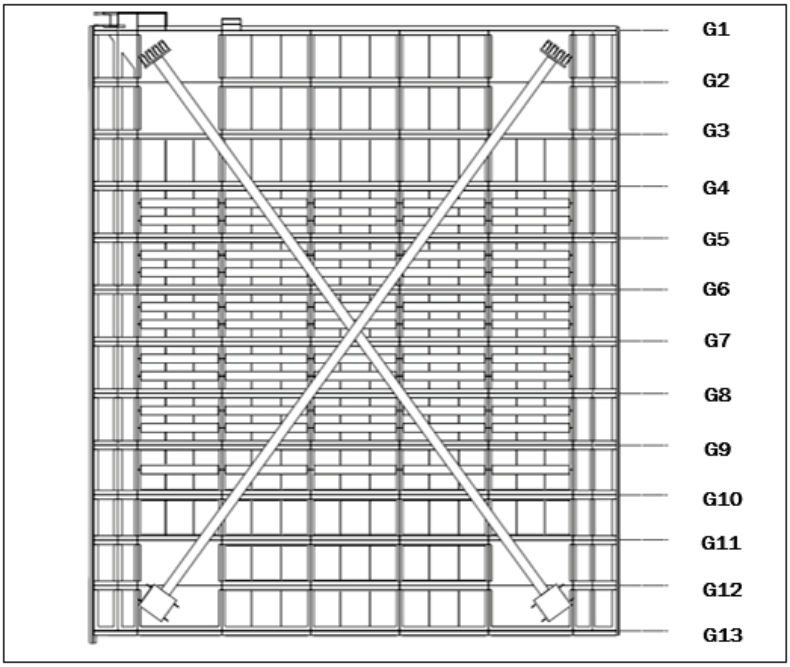

Figure 46. Results for Lock 27, no-gap scenario.

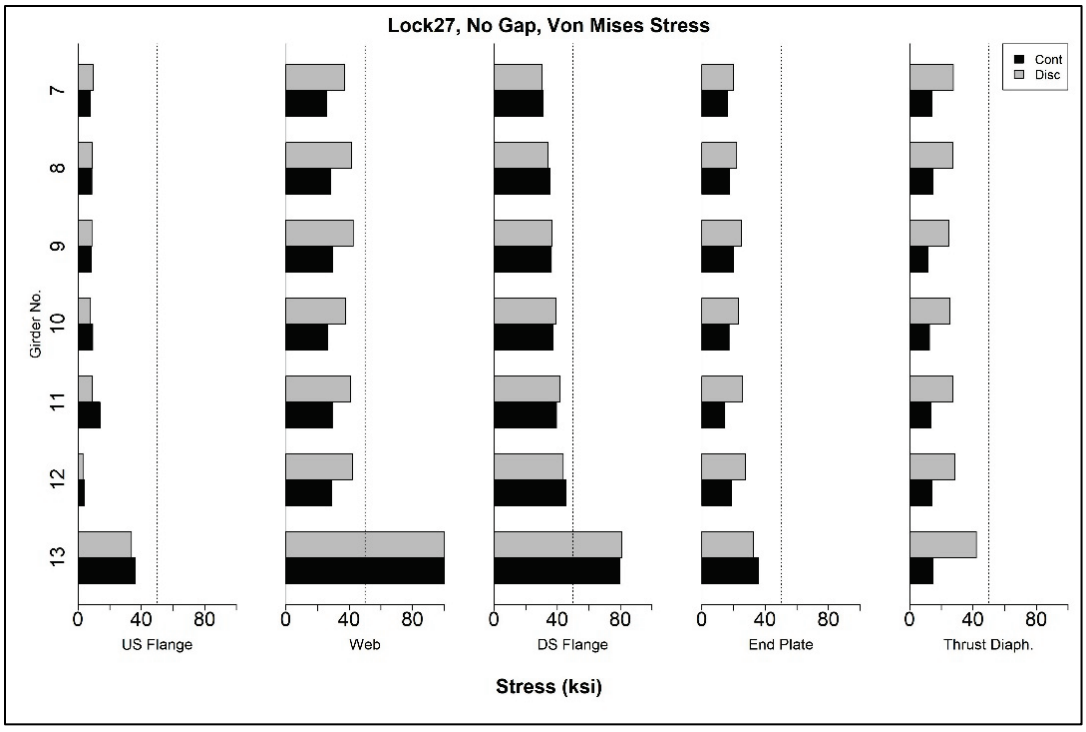

Figure 47. Results for Lock 27, low-gap scenario.

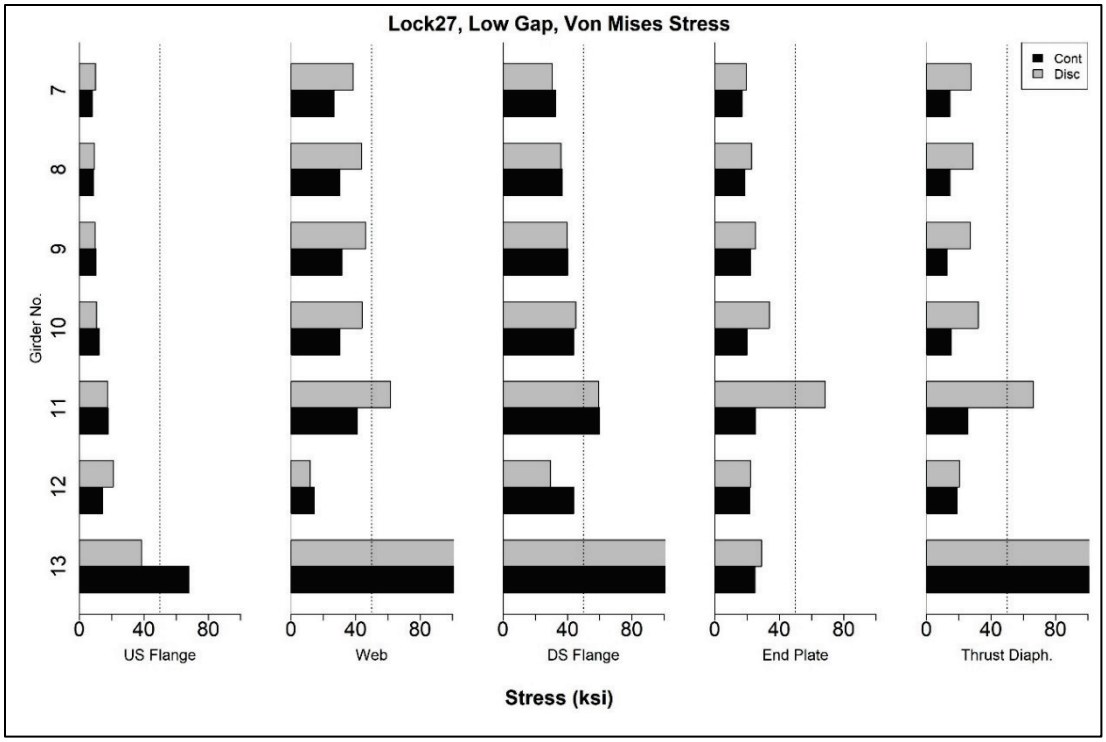

Figure 48. Results for Lock 27, mid-gap scenario.

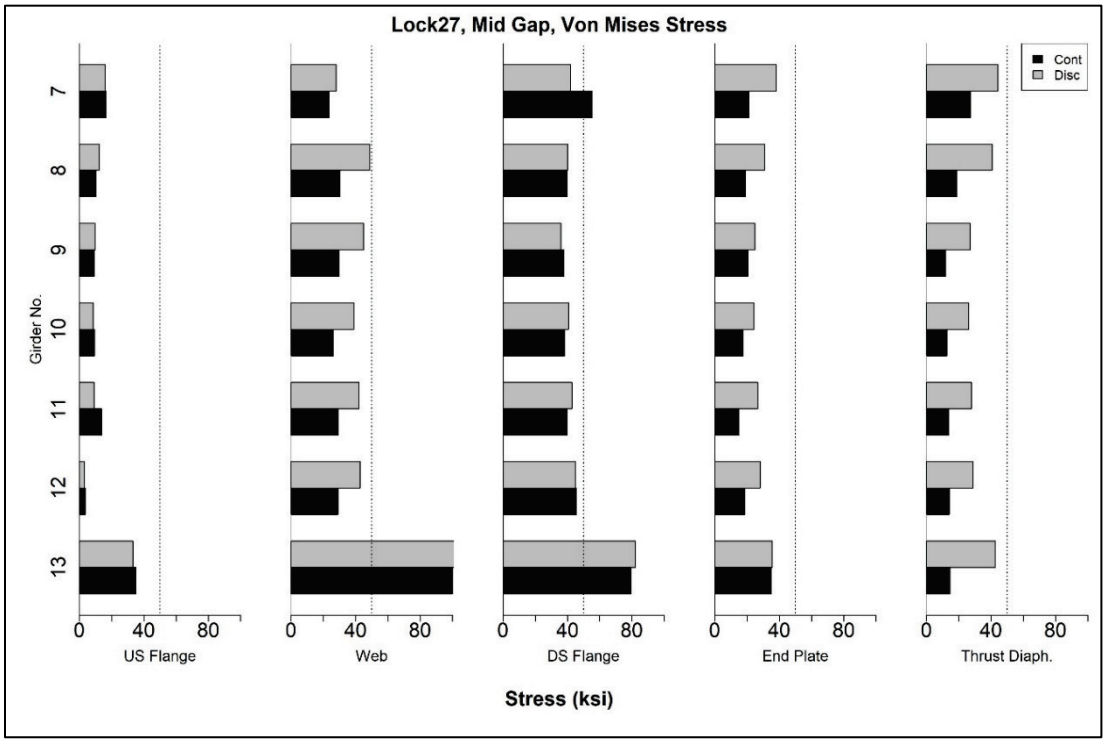

5 Discussion

This section first discusses results presented in Chapter 4 and then discusses general observations. It is emphasized again that the modeled results provided were for load cases that were, in general, extreme for the lock gates in question. For some of these cases (particularly Lock 27), the lock gate is not designed to withstand the loads imparted on the structure as modeled in the research presented here. However, the materials used in the finite element models were linear elastic, so the behavior of the actual gate is expected to be as good as or better than the behavior seen in the model.

5.1 Gate-specific results

Here, observations are made on the behavior of and stress redistribution in individual gates when comparing the use of discontinuous quoin blocks to continuous ones.

5.1.1 Lockport

The Lockport miter gate appears to be a very robust gate. In every case, the stress in locations of interest on the gate never surpassed 50 ksi. When comparing continuous and discontinuous block results, in general the stress appears to change very little in the girder flanges but changes most significantly in the vertical thrust diaphragms. For the no-gap and mid-gap scenarios, the highest stresses occur on the bottom girder, as expected. Note that the regions investigated on the bottom girder are near the complex pintle area, which is difficult to model accurately. For the low-gap scenario, the stresses significantly redistribute away from girder 13, accumulate in girders 10 and 11, and markedly decrease in girder 12. Interestingly, it appears that the stress in the low-gap scenario in girder 11 appears to increase when using continuous blocks (when compared to the no-gap case), but it appears to decrease when using discontinuous blocks. This phenomenon is reasonable because the low gap starts in a location between girders 10 and 11. Therefore, for the continuous block case, there is still some contact in the portion of quoin that is either influenced by or has influence on girder 11. When a discontinuous block is used, this influence is no longer the case. Given the results from the numerical simulations, discontinuous contact blocks appear to be a promising retrofit option for lock gates of similar design and with similar loads as the Lockport gate.

5.1.2 Terry

Terry is a relatively short gate by USACE standards, so the magnitude of loads imparted on the gate are relatively small compared to other gates that were modeled. Note that there were issues in obtaining a converged solution for the mid-gap scenario for Terry. Due to changes that had to be made in the model to obtain convergence, the results for the mid-gap scenario do not provide a one-to-one comparison for the other two scenarios. Nevertheless, the stress results for the Terry Lock and Dam were, with few exceptions, below 50 ksi. Notable exceptions are regions near the pintle (again, this area is difficult to accurately model) and the end plate in girder 9 for the low-gap scenario. The redistribution of stress in Terry appears to be fairly pronounced, with some regions increasing and some regions decreasing in stress. Terry is also a bit unusual in that it appears that for the no-gap scenario, the largest changes occur in the girder flanges. Given the results from the numerical simulations, discontinuous contact blocks appear to be a promising retrofit option for lock gates of similar design and with similar loads as the Terry gate.

5.1.3 Racine

The results for the Racine miter gate show significant changes in stress between the discontinuous and continuous block cases. Generally, the most significant changes in stress appear to occur at the thrust diaphragms of the girder, with much less significant changes occurring in the girder flanges. Nevertheless, for the no-gap and mid-gap scenarios, stresses are always below 50 ksi. For the low gap scenario, several locations in the quoin region have stress that surpass 50 ksi—particularly the upstream flange, web, and upper thrust of girder 13, and the upper thrust diaphragm of girder 10. Note that the pintle region of the gate is not accurately modeled in Abaqus because accurate modeling would be prohibitively difficult. When a low gap is introduced, the pintle takes much of the load, and the crudeness of the pintle region of the model leads to large stress concentrations in this region, whether continuous or discontinuous contact blocks are being considered. However, the change in stress is not significant, so it seems unlikely that the use of discontinuous contact blocks will negatively impact gate life. Nevertheless, given the results of the numerical models, discontinuous contact blocks may be a viable option for lock gates of similar design and with similar loads as Racine. However, it seems likely that additional retrofit procedures may need to be considered, particularly in the bottom girders.

The retrofit options may include the addition of stiffeners, doubler plates, or other structural components to redistribute load.

5.1.4 Cannelton

The Cannelton model (which represents a gate that has yet to be built) generally experienced very significant changes in stress when using discontinuous blocks, frequently on the order of a 200% increase. These changes in stress are most significant in the thrust diaphragms, but they are negligible in the flanges. For the mid-gap and low-gap scenarios, there are several areas of the bottom girder that are above 50 ksi, but this appears to occur in the continuous case as well, again suggesting that this is a symptom of poor pintle modeling and an extreme load case. For the low-gap scenario, there are very significant changes in stress in several locations on girder 10 and 11. For instance, the web and lower thrust diaphragm are above 50 ksi in the discontinuous case but are much less than 50 ksi in the continuous case. Again, this is caused by the proximity of the ends of girders 10 and 11 to the start of the modeled gap, so girder 10 needs to carry all the load that is unable to be carried by the lower girders. Given the results of the numerical models, discontinuous contact blocks may be a viable option for lock gates of similar design and with similar loads as Cannelton. However, additional retrofit procedures will likely need to be considered, as they were in the discussion of Racine (5.1.3). The stress concentration in the upper thrust plate of girder 10 is of particular concern in the low gap case.

5.1.5 Greenup

The results from the Greenup miter gate show that, in general, there is a decrease in stress in the flanges and an increase in stress elsewhere for each girder (with few exceptions). The largest increases in stress occur in the end plate and in the diaphragms. Nevertheless, there are very few regions of the gate that were above 50 ksi—most notably the end plate of girder 12 in the no-gap and mid-gap scenarios. Note that the stress in the end plate of girder 12 also is near or above 50 ksi in the continuous case. The downstream flange of girder 10 in the low-gap scenario decreases from above 50 ksi in the continuous case to just below 50 ksi in the discontinuous case. The upper thrust diaphragm of girder 10 in the low-gap scenario appears to significantly increase from well below 50 ksi to very near 50 ksi. Given the results from the numerical models, discontinuous contact blocks may be a viable option for lock gates of

similar design and with similar loads as Greenup. Again, additional retrofit procedures may need to be considered.

5.1.6 Lock 27

Lock 27 was designed to handle relatively low head loads compared to the gate's size, so this study's intended load on Lock 27 was too extreme. This led to great difficulty in getting the models to successfully run due to the nonlinear nature of contact analysis. As such, the imparted load had to be reduced significantly to obtain any results for Lock 27. Still, the load imparted on Lock 27 is somewhat extreme, as the gate appeared to almost never experience more than 10 ft of differential head. This is noted again because the results for Lock 27 are not directly comparable to the other modeled lock gates. Nevertheless, for the loads imparted on Lock 27, the changes in the stress field when using discontinuous contact blocks are acceptable. Like many of the other gates modeled, Lock 27 suffers from poor pintle modeling, so the excessive stresses in that region of the gate are likely a byproduct of the poor representation of the pintle. The most alarming changes in stress happen in girder 11 for the low-gap scenario, where the stress in the end plate and lower thrust diaphragm increases from well below 50 ksi to beyond 50 ksi. Given the results of the numerical models, discontinuous quoin blocks may be a viable option for locks of similar design and with similar loads as Lock 27 but similar to some of the gates above, additional retrofit procedures should be considered.

5.2 Localized nature of redistribution of stress

For the discontinuous quoin, stress tends to redistribute to higher concentrations in the web and diaphragm plates, and there is generally less change in the stress field in the flanges. Typical behavior near the quoin blocks is shown in Figure 49, Figure 50, Figure 51, and Figure 52. Large stress concentrations occur in locations where the quoin block corner meets the end plate. Plates near these locations, such as the web and thrust plates, also have stress concentrations. Moving farther from the quoin blocks, the stress quickly attenuates in the rest of the web. What appears to happen is that by using discontinuous quoin blocks, the stress that would otherwise be relatively evenly distributed in the thrust diaphragm is instead concentrated at locations where the discontinuous quoin block ends. Most of the rest of the diaphragm has very little stress. This finding makes sense, as the discontinuous quoin block pieces essentially act as supports for the diaphragms to behave as simply

supported beams between the block pieces; most of the stress occurring in these regions is shearing stress.

The localized nature of the stress concentrations in the discontinuous contact block case suggest that additional retrofit options could give discontinuous contact blocks further viability. Some possible retrofit options include adding additional bracing and stiffener plates, or similar to facilitate redistributing these stress concentrations to the rest of the gate. Indeed, the use of these options may disperse the stress more effectively than a continuous quoin block. Investigating these additional retrofit options is outside the scope of this report and will be left to future work.

Figure 49. Racine gates, von Mises results and area of interest for localization effects.

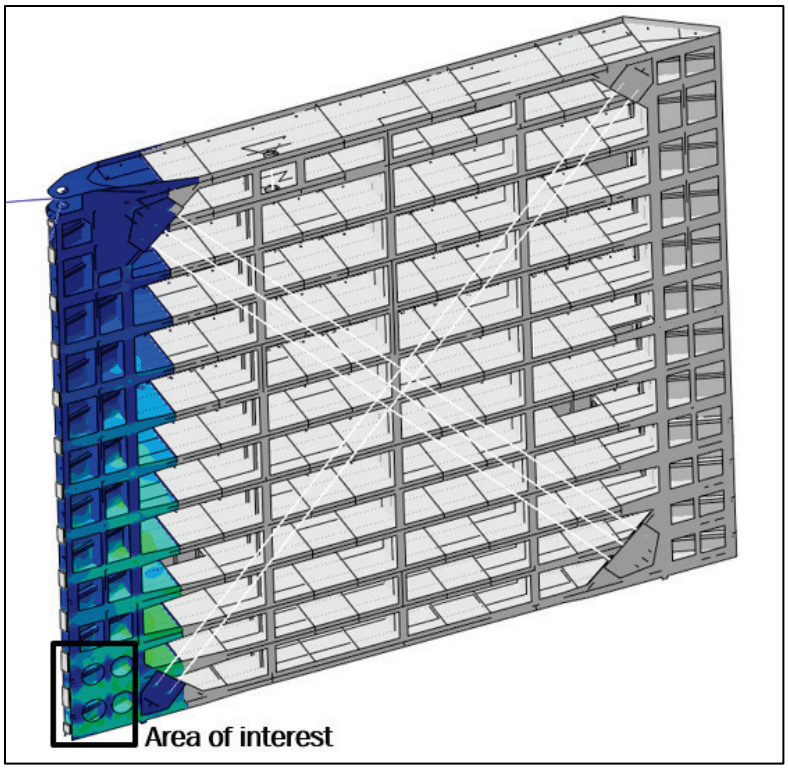

Figure 50. Localized stress in end plate immediately next to the end of the end plate.

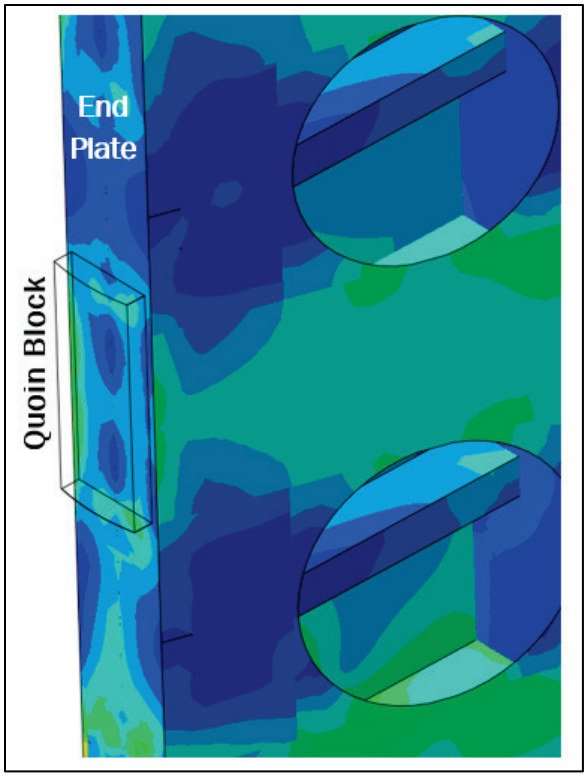

Figure 51. Localized stress concentration in a thrust diaphragm immediately next to the end of a discontinuous quoin piece.

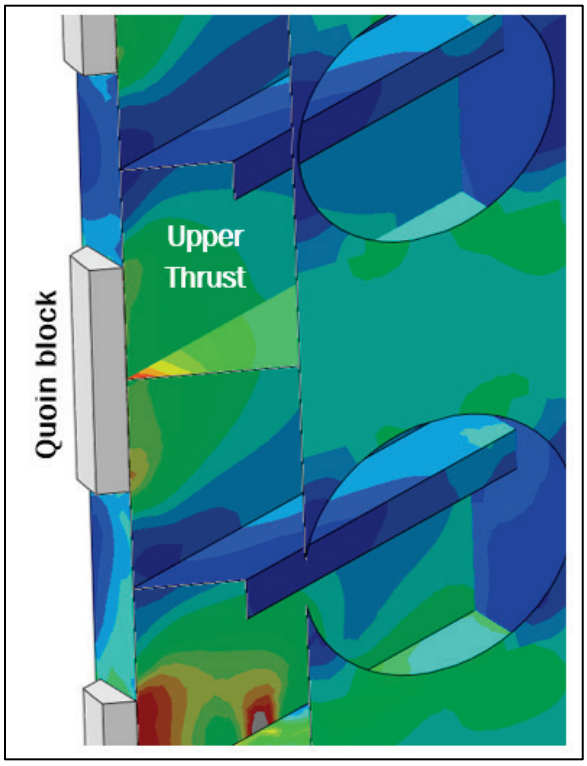

Figure 52. Localized stress concentration for discontinuous case in girder web next to corner of discontinuous block.

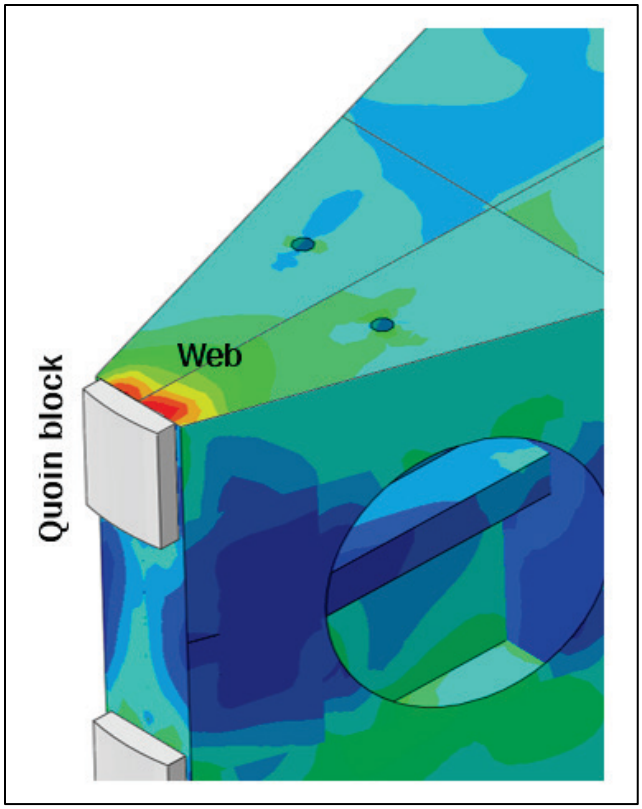

5.3 Fatigue

Even though most cases that this report considers do not exceed 50 ksi, they do significantly increase the stress in certain areas of the gate. This may decrease the fatigue life of the structure, particularly at the welds (James and Zhang 1996). One common measure of a material's resistance to fatigue is the S-N curve. The letter S stands for stress, and N stands for number of load cycles. The S-N curve for welds generally takes the following form:

$$N = \left(\frac{C}{\Delta S}\right)^m$$

where C and m are constants related to the material (Gurney 1979; Hobbacher 2016).This formula can be used to estimate the reduction in fatigue life from a discontinuous quoin block, based on the increases in stress displayed in Figure 24–Figure 48. Assuming that the stress in the quoin region is close to zero as the gate opens and closes, ΔS is the stress when the hydrostatic load is applied. A typical m value is 3 (Gurney 1979;

Hobbacher 2016). Taking a 100% increase in stress from the discontinuous quoin yields the following equation:

$$N_{disc}^{100\%} = \left(\frac{C}{2\Delta S}\right)^3 = \frac{1}{8}\left(\frac{C}{\Delta S}\right)^m = \frac{1}{8}N$$

Similarly for a 50% increase, the equation is as follows:

$$N_{disc}^{50\%} = \left(\frac{C}{1.5\Delta S}\right)^3 = \frac{1}{3.375}\left(\frac{C}{\Delta S}\right)^m = \frac{1}{3.375}N$$

A 100% increase in stress reduces the fatigue life by 87.5%, and a 50% increase in stress reduces fatigue life by 70.4%. This reduction is significant if the continuous quoin block has a short fatigue life. Thus, a full fatigue analysis of the gate is advisable for a discontinuous quoin retrofit. In that full analysis, a more comprehensive ΔS should be used that accounts for the gate gravity, opening, closing, and hydrostatic load.

6 Findings on Quoin Block Splice Location

The investigation into the quoin blocks revealed a peculiar requirement noted in the EM (USACE 1994) when quoin blocks are spliced. It states that if the contact blocks are assembled in pieces, splices should occur at the center lines of the horizontal girder. The exact wording of the EM is "…blocks are made up of 15- to 20-ft long section with transverse joints occurring at the center lines of horizontal girder webs" (USACE 1994). This suggestion appears to have readily been applied in practice, with many of the structural drawings used in this research having notes requiring contact block splices to occur at the center lines of the girders. One such example, shown in Figure 53, is a note on the Lock 27 drawing sheet for the quoin block, clearly stating that the splices shall be made in line with the girder web centerline.

Figure 53. Note on Lock 27 drawings calling for contact splices to occur at centerline of girder webs.

The investigation into discontinuous quoin blocks revealed that this suggestion is inappropriate and will likely lead to unnecessary stress concentration and potential issues with the quoin block itself. As shown in Figure 7 in the introduction of this report, the highest stresses in the contact-region of a miter gate are exactly in line with the center-lines of the girder webs. For convenient reference, Figure 7 is reproduced here as Figure 54, showing that maximum stress occurs at the girder center lines. This phenomenon seems to suggest that the likely best location for contact block splices would be as far from a girder centerline as possible.

Figure 54. Reproduction of Figure 7, showing the maximum von Mises stress is at the centerlines of the girders.

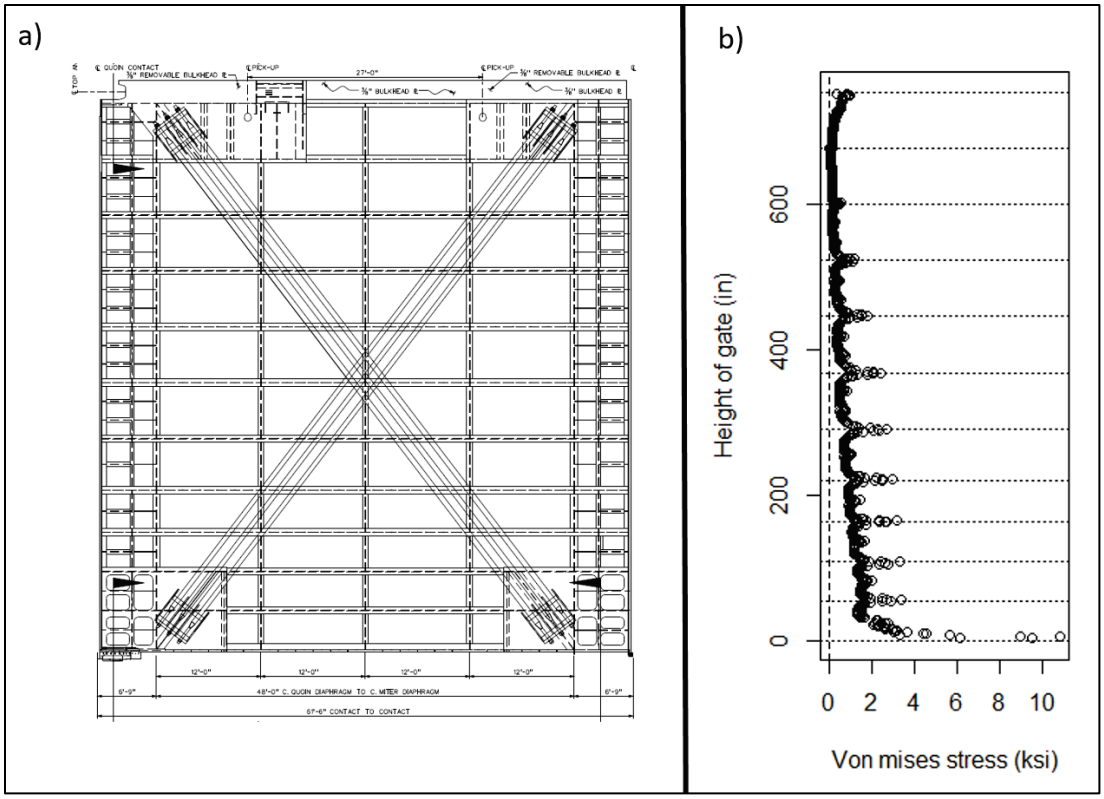

To validate the idea that contact splices should be as far as possible from a girder centerline, the splices are modeled as per the EM (USACE 1994) and structural drawing instructions. A splice is placed exactly at the contact block center line, such that the two contact block pieces are perfectly flush with each other. The results from different models show that this configuration, when compared to the no-splice case, leads to an increase in stress in the end plate and girder web immediately next to the splice on the order of 1 to 5 ksi. An example of this is shown in Figure 55, which shows a contour plot of the change in von Mises stress between the case with no splice and the case with a splice at the center line of the girder. In Figure 55, (a) shows the geometry of the splice, (b) removes the contact block pieces to show the change in stress in the end plate, and (c) shows the change in stress in the web plate immediately next to the splice. In the contour plot, green represents no change, red represents a positive change, and blue represents a negative change. As seen, there are increases in stress in several location when a splice is located in line with the girder web center-line.

Figure 55. (a) Perfectly flush splice located immediately next to girder web centerline; (b) increase in stress between splice and no splice case for end plate; (c) increase in stress for girder web.

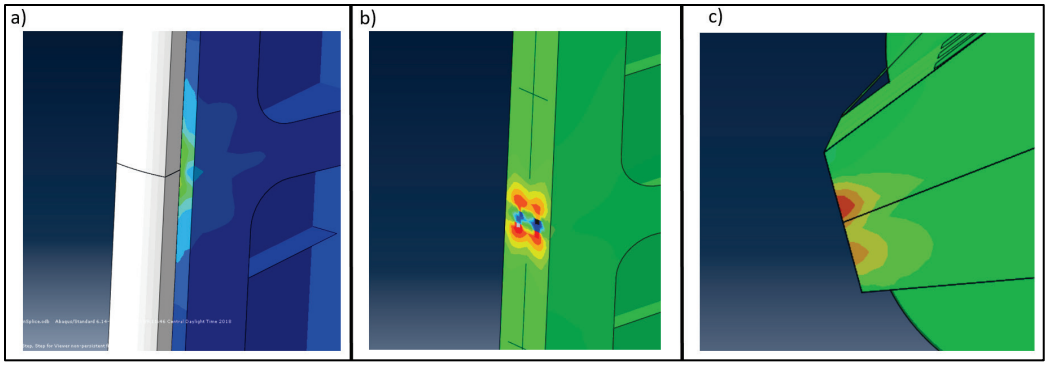

In contrast, an additional example is modeled that puts the splice midway between two girders for the same models. Results for this are shown in Figure 56. Figure 56(a) shows the geometry and location of the splice, (b) shows the change in stress in the end plate, and (c) shows the change in stress in the diaphragm. The contour limits and colors in Figure 56 are the same as in Figure 55. As can be seen, there is actually a decrease in stress in the end plate, and no discernable change in stress in the thrust diaphragm immediately next to the splice.

Figure 56. (a) Location of splice midway between girders, (b) decrease in stress in end plate, (c) no real change in stress in thrust diaphragm.

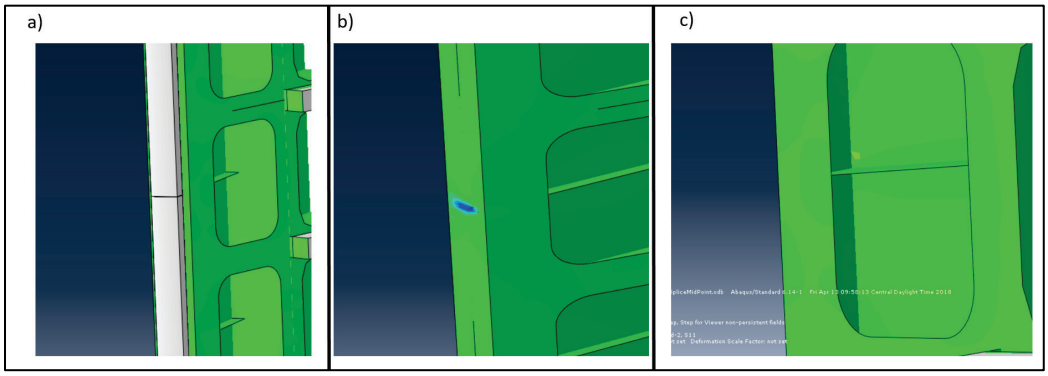

The results shown here assume perfect contact between the contact block and the gate's end plate. This assumption is questionable, particularly if an epoxy is used as the backing material for the quoin block. Given the typically low strength of epoxy, it seems likely that the epoxy would crack off in the splice region between the splice bolts. From these results, it is the researchers' opinion that contact block splice should never be placed in line with a girder web centerline but should be placed as far from the web centerline as possible.

7 Conclusions

The research presented herein investigates the feasibility of utilizing discontinuous contact blocks on miter gates. Of particular interest is the feasibility of utilizing these contact blocks as a retrofit option on already existing gates in the USACE inventory. To accomplish this investigation, finite element models were utilized for an array of representative miter gates in the USACE inventory. Model simulations were run using continuous contact blocks and discontinuous contact blocks, with the gate being subjected to an extreme load case. Furthermore, the sensitivity to damage of a gate with discontinuous quoin blocks was investigated by means of inducing boundary condition degradation in the form of gaps in the bearing surface of the quoin. The results showed varying degrees of applicability depending on which gate is investigated, as discussed below:

- **Lockport.** The Lockport gate appears to be fairly robust. The changes in the stress caused by the use of discontinuous blocks appears to be within the realm of acceptability. For lock gates of similar design, and subjected to similar loads, discontinuous contact blocks appear to be a promising retrofit option.
- **Terry.** The Terry gate appears to undergo very little change when discontinuous contact blocks are used when compared to other lock gates. Regions with high stress generally have high stress in both the continuous and discontinuous cases. Thus, for lock gates of similar design and subjected to similar loads, discontinuous contact blocks appear to be a promising retrofit option.
- **Racine.** Racine seems to undergo more significant changes when discontinuous contact blocks are used. While the magnitude of stress generally appears to be below 50 ksi (with the exception of some locations in the low gap scenario), the change in stress is significant, particularly if considering fatigue life. For lock gates of similar design and subjected to similar loads, discontinuous contact blocks may be a viable option, but additional retrofit procedures may need to be considered, particularly in the bottom girders. The retrofit options may include the addition of stiffeners and doubler plates, or other structural members to redistribute load.
- **Cannelton.** Cannelton underwent more significant changes in stress when discontinuous blocks were used. It is the researchers' opinion that the results at the bottom girder are not reasonable and are a byproduct of poor pintle modeling. While the magnitude of stress

generally appears to be below 50 ksi (with the exception of some locations in the low gap scenario), the large change in stress may decrease gate fatigue life. For lock gates of similar design and subjected to similar loads, discontinuous contact blocks may be a viable option, but additional retrofit procedures needs to be considered, as with Racine above. The stress concentration in the upper thrust plate of girder 10 is of particular concern in the low gap case.

- **Greenup.** Although not as severe as Racine or Cannelton, Greenup experienced significant changes in stress due to the use of discontinuous quoin blocks, particularly in the diaphragms of the quoin block region. Mainly, the stresses were well below 50 ksi, with few exceptions. It is reiterated here that the discontinuous contact blocks considered for Greenup consisted of contact block pieces at the end of each girder, as well as at the intermediate thrust plates. For lock gates of similar design and subjected to similar loads, discontinuous contact blocks may be a viable option, but additional retrofit procedures may need to be considered.
- **Lock 27.** The results for lock 27 show that, like many of the other gates, the changes in stress when using discontinuous quoin blocks are such that the stresses are mainly below 50 ksi, with few exceptions. For locks of similar design, and subject to similar loads, discontinuous quoin blocks may be a viable option, but additional retrofit procedures should be considered.

Generally speaking, discontinuous quoin blocks are clearly a viable option when lock gates are designed a priori to use them. Note once more that the loads used in this research are not very representative of what a lock gate would typically encounter and were intended to represent an extreme scenario. Furthermore, the length of the discontinuous quoin blocks investigated in this study (girder flange widths plus 2 in. of overhang) is fairly small. It is expected that, as the pieces of quoin block get longer, the discontinuous quoin block effectively converges towards a continuous quoin block, so the stress are expected to decrease with an increase in block piece size.

With these observations in mind, utilizing discontinuous quoin blocks is a promising retrofit option for USACE miter gates. However, the need for additional retrofit procedures needs to be investigated for each gate in which discontinuous quoin blocks are considered during the retrofit design phase. Additional retrofits may include bracing, doubler plates,

stiffener plates, or similar. These procedures should seek to reduce stress concentrations produced by the converging load paths at the discontinuous contact block. It is at the discretion of a design engineer to perform the required analysis to determine what, if any, additional retrofit options would be required on a gate-by-gate basis. It is the opinion of the researchers that a finite element model should be created for the gate to capture this complex stress behavior.

It would be beneficial for future work to investigate an optimal length of discontinuous quoin block piece and to investigate the effect of additional retrofit options that could add to the viability of the discontinuous quoin block. In addition, a rigorous investigation should be performed on each gate into the effect on fatigue life of gate components caused by the redistribution of stress due to the use of discontinuous contact blocks. These investigations are outside the scope of the research presented herein.

References

Daniel, R. A. 2000. "Mitre Gates in Some Recent Lock Projects in the Netherlands." *Stahlbau* 69(12): 952–964.

Dassault Systèmes (3DS). 2017. "Abaqus Documentation." https://www.3ds.com/support/documentation/

Eick, Brian A., Zachary R. Treece, Billie F. Spencer Jr., Matthew D. Smith, Steven C. Sweeney, Quincy G. Alexander, and Stuart D. Foltz. 2018. "Automated Damage Detection in Miter Gates of Navigation Locks." *Structural Control and Health Monitoring* 25(1): 32053. https://doi.org/10.1002/stc.2053

Gurney, Timothy R. 1979. *Fatigue of Welded Structures*. Revised edition. Cambridge, England: Cambridge University Press (CUP).

Hobbacher, A. F. 2016. "Fatigue Resistance." In *Recommendations for Fatigue Design of Welded Joints and Components*, 37–89, International Institute of Welding (IIW) series. Switzerland: Springer International Publishing.

James, R. J., and L. Zhang. 1996. *Fatigue Cracking Evaluation of the Markland Miter Gates*. ANATECH Report ANA-96-0201 to Corps of Engineers, Louisville District. San Diego, CA: ANATECH Corporation.

PIANC, InCom Working Group (WG). 2017. *Mitre Gate Design and Operation*. WG Report No. 154-2017. Brussels, Belgium: PIANC, the World Association of Waterborne Transport Infrastructure.

U.S. Army Corps of Engineers (USACE). 1994. *Lock Gates and Operating Equipment*. EM 1110-2-2703. Washington DC: Headquarters, U.S. Army Corps of Engineers.

USACE. 2014a. *Design of Hydraulic Steel Structures*. ETL 1110-2-584. Washington DC: Headquarters, U.S. Army Corps of Engineers.

USACE. 2014b. *Lock Characteristics General Report*. Vicksburg, MS: Vicksburg District, U.S. Army Corps of Engineers. http://cwbi-ndc-nav.s3-website-us-east-1.amazonaws.com/files/lpms/pdf/lkgenrl.pdf

USACE. 2016a. "Geographic Distribution of U.S. Waterway Facilities." Chart and lock facts in *The U.S. Waterway System: 2016 Transportation Facts and Information,* 4. Alexandria, VA: Navigation and Civil Works Decision Support Center (NDC), U.S. Army Corps of Engineers. https://usace.contentdm.oclc.org/utils/getfile/collection/p16021coll2/id/1829

USACE. 2016b. *Technologies to Extend the Life of Existing Infrastructure: Navigation Infrastructure* (Vol. 1). Vicksburg, MS: Vicksburg District, U.S. Army Corps of Engineers. https://operations.erdc.dren.mil/pdfs/TechExtLife1.pdf

Appendix A: Tabulated von Mises Stresses

For reference, this appendix provides the raw von Mises stress data that were used in the plots in Chapter 4, with no-gap, low-gap, and mid-gap scenarios for each location and for continuous and discontinuous block. Tables A1–A6 contain data for Lockport, Tables A7–A12 contain data for Racine, Tables A13–A18 contain data for Cannelton, Tables A19–BA24 contain data for Greenup, Tables A25–A30 contain information for Terry, and Tables A31–A36 contain data for Lock 26.

Lockport

No-gap scenario

Table A-1. von Mises stress (ksi), continuous block, no gap, Lockport.

	Location					
	US Flange	Web	DS Flange	End Plate	Upper Thrust	Lower Thrust
Girder 7	9.77	10.9	8.25	5.78	7.96	8.21
Girder 8	10.6	12.1	9.00	6.52	8.88	8.90
Girder 9	11.2	12.9	9.50	7.13	9.30	9.75
Girder 10	11.6	13.1	10.8	7.76	9.88	8.57
Girder 11	10.8	14.8	14.1	9.02	8.58	8.73
Girder 12	9.95	17.3	18.8	10.7	8.58	8.34
Girder 13	21.6	21.6	26.1	49.3	12.0	NA

Table A-2. von Mises stress (ksi), discontinuous block, no gap, Lockport.

	Location					
	US Flange	Web	DS Flange	End Plate	Upper Thrust	Lower Thrust
Girder 7	9.48	14.3	7.02	8.23	13.4	13.7
Girder 8	10.2	15.3	7.83	9.20	14.7	14.5
Girder 9	10.7	16.2	8.39	9.92	15.4	15.3
Girder 10	10.8	16.8	8.96	10.5	16.5	14.8
Girder 11	10.2	18.8	11.7	11.9	15.4	14.9
Girder 12	10.2	20.2	15.3	12.4	15.1	12.7
Girder 13	21.1	21.6	25.8	44.3	18.8	NA

Low-gap scenario

Table A-3. von Mises stress (ksi), continuous block, low gap, Lockport.

Location						
	US Flange	Web	DS Flange	End Plate	Upper Thrust	Lower Thrust
Girder 7	10.3	11.0	8.90	6.27	8.10	8.47
Girder 8	11.7	12.7	10.2	7.40	9.24	9.56
Girder 9	13.2	14.9	11.5	8.79	10.3	11.5
Girder 10	15.0	20.5	17.7	13.2	14.4	27.8
Girder 11	19.9	4.71	26.9	8.60	25.5	5.17
Girder 12	6.00	4.75	7.15	5.49	5.56	4.74
Girder 13	22.0	7.67	7.09	7.85	18.1	NA

Table A-4. von Mises stress (ksi), discontinuous block, low gap, Lockport.

Location						
	US Flange	Web	DS Flange	End Plate	Upper Thrust	Lower Thrust
Girder 7	9.76	15.2	7.90	8.98	14.2	14.5
Girder 8	11.1	17.8	9.47	10.8	16.1	16.5
Girder 9	12.9	21.4	11.2	13.1	18.4	21.1
Girder 10	17.6	32.7	17.1	24.6	26.7	42.8
Girder 11	12.4	4.56	13.9	8.77	14.4	6.30
Girder 12	6.00	5.47	8.94	9.53	8.68	7.46
Girder 13	23.7	10.7	7.20	9.34	27.6	NA

Mid-gap scenario

Table A-5. von Mises stress (ksi), continuous block, mid gap, Lockport.

Location						
	US Flange	Web	DS Flange	End Plate	Upper Thrust	Lower Thrust
Girder 7	9.78	10.9	8.36	5.84	8.00	8.23
Girder 8	10.7	12.1	9.10	6.43	8.90	8.90
Girder 9	11.2	12.8	9.50	7.16	9.30	9.76
Girder 10	11.6	13.1	10.9	7.76	9.88	8.57
Girder 11	10.8	14.8	14.1	9.00	8.58	8.72
Girder 12	9.94	17.3	18.8	10.7	8.55	8.32
Girder 13	21.6	21.6	26.1	49.3	11.98	NA

Table A-6. von Mises stress (ksi), discontinuous block, mid gap Lockport.

Location						
	US Flange	Web	DS Flange	End Plate	Upper Thrust	Lower Thrust
Girder 7	9.51	14.4	7.14	8.33	13.5	13.8
Girder 8	10.2	15.4	7.91	9.25	14.7	14.5
Girder 9	10.7	16.3	8.45	9.96	15.4	15.3
Girder 10	10.8	16.9	8.95	10.6	16.5	14.8
Girder 11	10.1	18.8	11.8	11.9	15.4	14.8
Girder 12	11.6	20.2	15.4	12.4	15.1	12.7
Girder 13	21.1	21.9	25.7	44.7	18.7	NA

Racine

No-gap scenario

Table A-7. von Mises stress (ksi), continuous block, no gap, Racine.

	Location					
	US Flange	Web	DS Flange	End Plate	Upper Thrust	Lower Thrust
Girder 7	10.6	19.3	10.2	5.30	12.6	13.3
Girder 8	11.4	22.2	11.0	6.20	14.9	15.3
Girder 9	14.2	24.5	12.9	8.70	16.7	11.2
Girder 10	13.0	21.1	13.0	10.4	11.6	11.9
Girder 11	18.1	24.7	18.9	11.5	12.3	11.7
Girder 12	18.1	25.4	20.3	16.4	14.9	13.0
Girder 13	29.4	50.5	29.6	37.0	31.9	NA

Table A-8. von Mises stress (ksi), discontinuous block, no gap, Racine.

	Location					
	US Flange	Web	DS Flange	End Plate	Upper Thrust	Lower Thrust
Girder 7	11.8	21.1	10.7	10.3	21.7	25.1
Girder 8	13.3	23.6	11.5	11.3	27.1	28.2
Girder 9	13.6	23.8	12.6	15.9	29.3	23.6
Girder 10	13.5	21.3	12.0	15.9	22.4	21.7
Girder 11	19.2	24.6	18.7	16.8	23.4	21.5
Girder 12	17.1	32.2	20.7	22.4	20.8	26.6
Girder 13	18.4	56.8	26.7	36.5	39.7	NA

Low gap scenario

Table A-9. von Mises stress (ksi), continuous block, low gap, Racine.

	Location					
	US Flange	Web	DS Flange	End Plate	Upper Thrust	Lower Thrust
Girder 7	13.6	22.7	13.1	7.30	14.3	15.5
Girder 8	18.0	28.2	16.0	8.90	17.6	19.1
Girder 9	25.7	33.8	22.4	11.9	21.4	18.2
Girder 10	33.1	32.0	32.7	29.8	38.3	26.6
Girder 11	24.7	22.4	36.3	15.8	26.1	14.2
Girder 12	6.20	18.0	25.7	8.00	9.60	15.6
Girder 13	76.3	391	8.10	7.30	192	NA

Table A-10. von Mises stress (ksi), discontinuous block, low gap, Racine.

	Location					
	US Flange	Web	DS Flange	End Plate	Upper Thrust	Lower Thrust
Girder 7	14.4	28.1	14.3	9.80	26.7	29.1
Girder 8	19.3	34.5	17.5	13.0	35.4	37.9
Girder 9	25.3	46.0	21.7	19.0	46.0	47.3
Girder 10	38.8	26.4	35.1	39.9	89.0	33.1
Girder 11	19.7	21.0	30.6	15.6	24.6	13.9
Girder 12	6.70	17.4	22.2	14.8	12.0	15.4
Girder 13	82.8	418	8.40	13.7	206	NA

Mid-gap scenario

Table A-11. von Mises stress (ksi), continuous block, mid gap, Racine.

	Location					
	US Flange	Web	DS Flange	End Plate	Upper Thrust	Lower Thrust
Girder 7	10.8	19.6	10.4	4.80	12.6	13.3
Girder 8	12.1	22.3	11.1	5.50	14.9	15.2
Girder 9	14.2	24.6	13.0	6.70	16.7	11.0
Girder 10	13.9	21.1	13.1	7.80	11.7	11.8
Girder 11	19.3	24.7	18.8	10.7	12.1	11.5
Girder 12	17.9	25.0	20.3	15.0	12.9	14.5
Girder 13	29.5	52.6	29.5	33.9	31.8	NA

Table A-12. von Mises stress (ksi), discontinuous block, mid gap, Racine.

	Location					
	US Flange	Web	DS Flange	End Plate	Upper Thrust	Lower Thrust
Girder 7	12.1	22.2	11.1	7.80	22.4	25.5
Girder 8	13.5	24.7	11.8	9.00	27.6	28.8
Girder 9	13.8	24.6	12.8	10.7	30.0	23.5
Girder 10	13.5	22.5	12.1	12.3	21.2	21.4
Girder 11	19.2	24.7	18.7	15.1	23.1	20.9
Girder 12	17.1	31.7	20.7	20.3	21.1	27.6
Girder 13	18.3	57.2	26.4	38.8	37.2	NA

Cannelton

No-gap scenario

Table A-13. von Mises stress (ksi), continuous block, no gap, Cannelton.

	Location					
	US Flange	Web	DS Flange	End Plate	Upper Thrust	Lower Thrust
Girder 7	11.9	9.80	12.1	6.06	6.67	7.25
Girder 8	13.4	11.9	12.6	7.20	7.90	8.60
Girder 9	13.6	13.6	13.4	8.27	9.20	9.50
Girder 10	14.2	14.9	13.2	8.70	9.80	10.5
Girder 11	13.0	15.9	17.1	9.50	10.6	11.4
Girder 12	9.37	18.9	22.1	14.2	11.2	12.2
Girder 13	7.09	28.6	38.8	23.5	12.1	14.5
Girder 14	41.4	91.4	75.4	91.2	25.2	NA

Table A-14. von Mises stress (ksi), discontinuous block, no gap, Cannelton.

	Location					
	US Flange	Web	DS Flange	End Plate	Upper Thrust	Lower Thrust
Girder 7	11.7	19.2	12.5	14.7	19.8	20.9
Girder 8	12.7	23.5	13.4	16.1	23.7	24.4
Girder 9	13.4	24.9	13.7	18.0	26.8	25.5
Girder 10	13.7	27.9	14.2	19.3	27.7	27.1
Girder 11	13.9	28.8	16.7	19.9	29.9	28.1
Girder 12	12.4	33.8	20.7	24.0	32.3	29.1
Girder 13	10.0	42.6	34.4	33.5	34.6	25.9
Girder 14	42.3	101	74.8	97.9	45.9	NA

Low-gap scenario

Table A-15. von Mises stress (ksi), continuous block, low gap, Cannelton.

	Location					
	US Flange	Web	DS Flange	End Plate	Upper Thrust	Lower Thrust
Girder 7	12.9	10.8	13.6	6.06	6.78	7.66
Girder 8	15.3	14.1	15.6	7.71	8.40	9.50
Girder 9	17.1	18.9	18.9	10.9	11.0	12.7
Girder 10	17.6	27.6	27.4	18.9	16.6	25.1
Girder 11	27.1	26.5	46.3	26.7	33.8	18.6
Girder 12	7.01	3.70	28.9	8.55	15.9	8.30
Girder 13	17.3	3.20	16.1	9.90	7.90	7.44
Girder 14	13.4	56.1	10.8	25.5	12.6	NA

Table A-16. von Mises stress (ksi), discontinuous block, low gap, Cannelton.

	Location					
	US Flange	Web	DS Flange	End Plate	Upper Thrust	Lower Thrust
Girder 7	12.4	22.2	13.1	16.5	21.9	22.8
Girder 8	14.3	29.1	17.3	20.7	27.7	29.4
Girder 9	17.3	35.6	20.3	25.2	35.2	37.6
Girder 10	23.5	50.9	29.1	37.7	45.1	59.4
Girder 11	20.7	44.8	36.9	36.2	49.7	33.5
Girder 12	7.80	4.60	28.1	11.1	14.8	7.70
Girder 13	15.7	5.03	16.3	14.3	13.7	13.1
Girder 14	11.3	62.4	18.1	22.9	19.8	NA

Mid-gap scenario

Table A-17. von Mises stress (ksi), continuous block, mid gap, Cannelton.

	Location					
	US Flange	Web	DS Flange	End Plate	Upper Thrust	Lower Thrust
Girder 7	11.4	9.50	12.2	4.88	6.90	7.26
Girder 8	12.7	10.9	12.4	6.50	7.76	8.33
Girder 9	12.8	12.5	13.0	7.70	8.80	8.80
Girder 10	12.3	14.0	12.8	7.80	9.20	9.78
Girder 11	12.2	15.4	16.6	8.50	9.90	10.6
Girder 12	8.30	18.7	21.1	13.8	10.7	11.3
Girder 13	3.80	26.7	36.4	22.5	11.2	12.7
Girder 14	37.2	86.7	69.9	86.5	22.4	NA

Table A-18. von Mises stress (ksi), discontinuous block, mid gap, Cannelton.

	Location					
	US Flange	Web	DS Flange	End Plate	Upper Thrust	Lower Thrust
Girder 7	12.1	22.5	13.9	16.6	24.3	23.6
Girder 8	12.9	25.3	14.4	17.3	25.5	25.6
Girder 9	13.5	25.9	14.4	18.7	27.7	26.1
Girder 10	13.7	28.6	14.7	19.6	28.2	27.4
Girder 11	13.9	29.2	16.9	20.4	30.1	28.4
Girder 12	12.4	33.9	20.7	24.2	32.3	29.2
Girder 13	10.0	42.6	34.5	33.6	34.5	26.5
Girder 14	42.2	100	74.4	58.5	45.7	NA

Greenup

No-gap scenario

Table A-19. von Mises stress (ksi), continuous block, no gap, Greenup.

Location						
	US Flange	Web	DS Flange	End Plate	Upper Thrust	Lower Thrust
Girder 7	21.6	13.1	25.8	9.70	11.0	11.2
Girder 8	23.6	14.9	28.3	10.8	12.7	12.7
Girder 9	24.8	16.4	28.8	11.2	13.6	13.2
Girder 10	25.2	17.5	32.1	11.9	14.1	14.2
Girder 11	32.8	20.9	36.5	29.4	14.2	14.4
Girder 12	25.6	22.6	31.6	13.0	13.9	15.2
Girder 13	15.0	27.6	34.5	49.0	20.6	NA

Table A-20. von Mises stress (ksi), discontinuous block, no gap, Greenup.

Location						
	US Flange	Web	DS Flange	End Plate	Upper Thrust	Lower Thrust
Girder 7	19.4	16.5	21.9	11.0	14.8	18.2
Girder 8	21.4	19.2	25.5	16.9	19.9	19.4
Girder 9	22.3	21.2	25.0	19.0	21.2	20.7
Girder 10	21.6	21.0	28.8	19.8	20.8	22.4
Girder 11	24.9	22.1	34.7	30.2	20.9	23.2
Girder 12	21.1	22.6	30.8	22.2	21.6	25.6
Girder 13	12.8	28.7	36.0	52.7	28.2	NA

Low-gap scenario

Table A-21. von Mises stress (ksi), continuous block, low gap, Greenup.

	Location					
	US Flange	Web	DS Flange	End Plate	Upper Thrust	Lower Thrust
Girder 7	22.6	13.8	26.4	10.0	11.0	11.6
Girder 8	25.7	16.0	29.6	11.6	12.9	13.4
Girder 9	29.5	18.3	33.7	13.0	14.7	15.2
Girder 10	34.7	22.7	45.4	22.4	19.1	29.2
Girder 11	35.4	18.2	54.8	20.6	25.8	15.9
Girder 12	9.30	9.60	13.9	10.1	10.0	12.0
Girder 13	21.2	31.9	35.4	25.4	35.4	NA

Table A-22. von Mises stress (ksi), discontinuous block, low gap, Greenup.

	Location					
	US Flange	Web	DS Flange	End Plate	Upper Thrust	Lower Thrust
Girder 7	20.2	16.8	22.7	13.6	15.5	16.6
Girder 8	22.4	20.0	27.2	21.7	20.2	22.2
Girder 9	26.4	24.6	29.3	25.9	26.3	26.5
Girder 10	27.6	33.6	40.7	40.0	31.4	46.2
Girder 11	28.9	22.3	45.5	43.3	49.8	15.4
Girder 12	10.5	9.20	15.8	26.5	19.6	17.4
Girder 13	23.0	34.0	32.5	24.2	38.2	NA

Mid-gap scenario

Table A-23. von Mises Stress (ksi), continuous block, mid gap, Greenup.

	Location					
	US Flange	Web	DS Flange	End Plate	Upper Thrust	Lower Thrust
Girder 7	22.5	13.8	26.6	10.2	11.6	11.6
Girder 8	23.9	15.2	28.7	11.0	13.0	12.9
Girder 9	24.9	16.6	29.1	11.3	13.7	13.2
Girder 10	25.2	17.7	32.3	11.9	14.2	14.3
Girder 11	32.7	21.0	36.6	29.4	14.2	14.4
Girder 12	25.6	22.6	31.6	13.0	13.9	15.4
Girder 13	12.7	27.5	34.4	51.4	20.6	NA

Table A-24. von Mises stress (ksi), discontinuous block, mid gap, Greenup.

	Location					
	US Flange	Web	DS Flange	End Plate	Upper Thrust	Lower Thrust
Girder 7	20.7	18.0	23.1	14.4	17.4	16.1
Girder 8	22.5	19.9	26.1	19.3	20.6	22.0
Girder 9	22.5	21.5	25.3	21.3	22.9	21.7
Girder 10	21.6	21.2	29.1	21.2	22.0	24.5
Girder 11	24.8	22.2	34.9	30.2	21.6	25.3
Girder 12	21.1	22.6	30.8	22.1	22.1	27.0
Girder 13	12.6	28.5	35.9	52.4	28.1	NA

Terry

No-gap scenario

Table A-25. von Mises stress (ksi), continuous block, no gap, Terry.

	Location					
	US Flange	Web	DS Flange	End Plate	Upper Thrust	Lower Thrust
Girder 6	6.24	25.3	23.3	14.3	7.12	6.83
Girder 7	6.15	27.9	26.7	16.5	7.91	7.64
Girder 8	5.98	32.2	24.3	18.4	6.60	7.01
Girder 9	2.58	30.2	32.7	19.9	6.43	9.03
Girder 10	14.6	49.2	50.1	49.5	11.7	NA

Table A-26. von Mises stress (ksi), discontinuous block, no gap, Terry.

	Location					
	US Flange	Web	DS Flange	End Plate	Upper Thrust	Lower Thrust
Girder 6	7.66	24.3	18.7	13.4	6.54	6.50
Girder 7	7.38	26.8	21.3	16.1	7.31	7.38
Girder 8	7.76	30.5	20.0	20.4	6.03	6.44
Girder 9	3.39	31.4	29.1	22.9	6.01	8.72
Girder 10	10.9	47.2	44.9	36.0	13.5	NA

Low-gap scenario

Table A-27. von Mises stress (ksi), continuous block, low gap, Terry.

	Location					
	US Flange	Web	DS Flange	End Plate	Upper Thrust	Lower Thrust
Girder 6	7.39	20.2	22.3	12.2	7.34	7.19
Girder 7	7.02	20.7	25.9	14.0	8.22	8.12
Girder 8	8.03	27.8	26.0	18.9	6.76	7.33
Girder 9	9.76	40.4	40.8	25.3	7.06	6.46
Girder 10	21.5	22.0	24.4	7.00	23.5	NA

Table A-28. von Mises stress (ksi), discontinuous block, low gap, Terry.

	Location					
	US Flange	Web	DS Flange	End Plate	Upper Thrust	Lower Thrust
Girder 6	7.63	27.4	20.0	14.1	6.72	6.73
Girder 7	8.28	31.0	22.8	17.3	7.53	8.06
Girder 8	9.79	37.7	23.8	23.8	6.20	6.56
Girder 9	9.83	24.3	42.8	52.5	7.12	7.30
Girder 10	20.2	24.3	16.8	5.13	26.3	NA

Mid-gap scenario

Table A-29. von Mises stress (ksi), continuous block, mid gap, Terry.

	Location					
	US Flange	Web	DS Flange	End Plate	Upper Thrust	Lower Thrust
Girder 6	13.6	16.5	20.4	13.1	9.70	9.40
Girder 7	9.40	18.0	21.9	15.5	9.80	9.70
Girder 8	8.80	18.7	23.5	16.3	9.80	10.0
Girder 9	9.00	20.1	31.1	18.2	9.13	9.80
Girder 10	28.9	42.5	38.8	60.8	8.50	NA

Table A-30. von Mises stress (ksi), discontinuous block, mid gap, Terry.

	Location					
	US Flange	Web	DS Flange	End Plate	Upper Thrust	Lower Thrust
Girder 6	14.4	25.6	16.1	22.1	24.3	16.8
Girder 7	10.7	25.6	18.3	21.6	15.9	15.2
Girder 8	10.6	25.8	18.9	22.3	16.0	15.7
Girder 9	7.10	26.6	26.3	24.6	16.2	14.9
Girder 10	24.8	47.1	39.4	56.6	16.1	NA

Lock 27

No-gap scenario

Table A-31. von Mises stress (ksi), continuous block, no gap, Lock 27.

Location						
	US Flange	Web	DS Flange	End Plate	Upper Thrust	Lower Thrust
Girder 7	7.60	25.6	31.3	16.1	11.9	13.9
Girder 8	8.70	28.2	35.3	17.5	14.5	11.1
Girder 9	8.30	29.3	36.4	20.2	10.9	11.7
Girder 10	9.30	26.1	37.5	17.3	11.8	12.5
Girder 11	13.7	29.2	39.6	14.5	12.6	13.6
Girder 12	3.80	28.9	45.5	18.6	13.8	14.2
Girder 13	35.8	99.9	79.7	35.7	14.5	NA

Table A-32. von Mises stress (ksi), discontinuous block, no gap, Lock 27.

Location						
	US Flange	Web	DS Flange	End Plate	Upper Thrust	Lower Thrust
Girder 7	**9.40**	**37.1**	**30.4**	**20.1**	**25.5**	**27.6**
Girder 8	8.90	41.5	34.2	22.2	27.2	24.6
Girder 9	8.60	42.4	36.6	24.9	24.7	23.7
Girder 10	7.90	37.5	39.1	23.3	24.9	25.2
Girder 11	8.90	40.9	41.7	25.9	25.7	27.2
Girder 12	3.10	41.9	43.9	27.5	28.5	27.3
Girder 13	33.8	99.8	80.6	32.6	42.1	NA

Low-gap scenario

Table A-33. von Mises stress (ksi), Lock 27, continuous, low gap.

	Location					
	US Flange	Web	DS Flange	End Plate	Upper Thrust	Lower Thrust
Girder 7	8.00	26.5	32.5	16.8	12.1	14.5
Girder 8	8.70	29.9	36.7	18.7	14.6	11.5
Girder 9	10.1	31.4	40.0	22.1	11.3	12.6
Girder 10	12.3	30.2	43.9	20.1	13.0	15.3
Girder 11	17.8	41.1	60.0	25.2	19.5	25.5
Girder 12	14.4	14.3	43.9	21.8	19.1	9.60
Girder 13	68.0	149	117	24.9	121	NA

Table A-34. von Mises stress (ksi), Lock 27, discontinuous, low gap.

	Location					
	US Flange	Web	DS Flange	End Plate	Upper Thrust	Lower Thrust
Girder 7	9.90	38.5	30.5	19.4	26.8	27.6
Girder 8	9.20	43.8	36.0	22.8	28.8	24.9
Girder 9	9.60	46.2	39.7	25.1	27.1	25.1
Girder 10	10.5	43.9	45.2	33.8	28.9	32.1
Girder 11	17.6	61.7	59.4	68.5	38.7	66.2
Girder 12	20.9	11.8	29.3	22.3	20.3	10.1
Girder 13	38.5	156	120	29.1	126	NA

Mid-gap scenario

Table A-35. von Mises stress (ksi), Lock 27, continuous, mid gap.

Location						
	US Flange	Web	DS Flange	End Plate	Upper Thrust	Lower Thrust
Girder 7	16.4	23.6	55.3	21.1	12.9	27.3
Girder 8	10.1	30.4	39.8	18.9	18.6	11.9
Girder 9	9.10	29.8	37.8	20.5	11.7	11.9
Girder 10	9.50	26.2	38.2	17.5	12.2	12.7
Girder 11	13.7	29.2	39.8	15.0	12.9	13.6
Girder 12	3.80	29.0	45.6	18.7	13.8	14.2
Girder 13	35.1	99.9	79.6	35.2	14.5	NA

Table A-36. von Mises stress (ksi), Lock 27, discontinuous, mid gap.

Location						
	US Flange	Web	DS Flange	End Plate	Upper Thrust	Lower Thrust
Girder 7	16.1	27.8	42.0	38.1	17.7	44.3
Girder 8	12.3	48.9	40.1	30.9	40.8	29.5
Girder 9	9.70	44.9	35.9	25.0	26.9	25.5
Girder 10	8.40	38.9	40.6	24.3	25.8	26.2
Girder 11	9.10	42.0	42.8	26.7	26.3	27.9
Girder 12	3.20	42.8	44.8	28.1	28.9	27.7
Girder 13	33.2	101.8	82.1	35.7	42.7	NA

Unit Conversion Factors

Multiply	By	To Obtain
feet	0.3048	meters
foot-pounds force	1.355818	joules
inches	0.0254	meters
pounds (mass)	0.45359237	kilograms
pounds (force) per square inch	6.894757	kilopascals
pounds (mass) per cubic foot	16.01846	kilograms per cubic meter
square inches	6.4516 E-04	square meters

REPORT DOCUMENTATION PAGE

Form Approved
OMB No. 0704-0188

1. REPORT DATE (DD-MM-YYYY)
July 2019

2. REPORT TYPE
Final

3. DATES COVERED (From - To)

4. TITLE AND SUBTITLE
Feasibility of Discontinuous Quoin Blocks for USACE Miter Gates

5a. CONTRACT NUMBER

5b. GRANT NUMBER

5c. PROGRAM ELEMENT NUMBER

6. AUTHOR(S)
Brian A. Eick, Matthew D. Smith, and Travis B. Fillmore

5d. PROJECT NUMBER

5e. TASK NUMBER

5f. WORK UNIT NUMBER
055F4K

7. PERFORMING ORGANIZATION NAME(S) AND ADDRESS(ES)
U.S. Army Engineer Research and Development Center
Construction Engineering Research Laboratory
PO Box 9005
Champaign, IL 61826-9005

U.S. Army Engineer Research and Development Center
Coastal and Hydraulics Laboratory
3909 Halls Ferry Road
Vicksburg, MS 39180-6199

8. PERFORMING ORGANIZATION REPORT NUMBER
ERDC TR-19-16

9. SPONSORING / MONITORING AGENCY NAME(S) AND ADDRESS(ES)
Headquarters, U.S. Army Corps of Engineers
441 G Street NW
Washington DC 20314-1000

10. SPONSOR/MONITOR'S ACRONYM(S)
HQUSACE

11. SPONSOR/MONITOR'S REPORT NUMBER(S)

12. DISTRIBUTION / AVAILABILITY STATEMENT
Approved for public release; distribution is unlimited.

13. SUPPLEMENTARY NOTES

14. ABSTRACT

Navigation lock chambers have gates that act both as damming surfaces for water and as doorways for vessels to enter and exit. Miter gates are by far the most common type of lock gate in the U.S. Army Corps of Engineers inventory. Horizontally framed miter gates are designed to bear continuously against the lock chamber wall along the height of the gate in the region known as the quoin. To aid continuous contact along the quoin, contact blocks are installed. Currently, each contact block is effectively one continuous piece of steel, making installation difficult and requiring the entire piece to be replaced even if only part is damaged. To address these shortcomings, this study investigated using discontinuous multiple quoin blocks instead, particularly as a retrofit option. Numerical models demonstrated the new design's stress range to be within appropriate limits, making discontinuous quoin blocks a feasible design. Supplementary results indicated issues with current placement of quoin block splices, suggesting that contact block splices should not be made in line with the centerline of girder webs as is common practice.

15. SUBJECT TERMS
Locks (Hydraulic engineerinf)—Maintenance and repair, Hydraulic gates, Hydraulic structures

16. SECURITY CLASSIFICATION OF:			17. LIMITATION OF ABSTRACT	18. NUMBER OF PAGES	19a. NAME OF RESPONSIBLE PERSON
					Brian A. Eick
a. REPORT	b. ABSTRACT	c. THIS PAGE			19b. TELEPHONE NUMBER
Unclassified	Unclassified	Unclassified	SAR	88	217-373-4432